Electronic Supplementary Information

"Twisted" Conjugated Molecules as Donor Materials for Efficient All-Small-Molecule Organic Solar Cells Processed with Tetrahydrofuran

Xiafei Cheng,[a] Miaomiao Li,*[a,b] Ziqi Guo,[d] Jinde Yu,[e] Guanghao Lu,[e] Laju Bu,[e] Long Ye,[f] Harald Ade,[f] Yongsheng Chen,*[d] and Yanhou Geng*[a,b,c]

[a] School of Materials Science and Engineering, Tianjin University, Tianjin 300072, P. R. China

[b] Tianjin Key Laboratory of Molecular Optoelectronic Science, Tianjin University, and Collaborative Innovation Center of Chemical Science and Engineering (Tianjin)

[c] Joint School of National University of Singapore and Tianjin University, International Campus of Tianjin University, Binhai New City, Fuzhou 350207, P. R. China

[d] The Key Laboratory of Functional Polymer Materials, State Key Laboratory and Institute of Elemento-Organic Chemistry, Centre of Nanoscale Science and Technology, College of Chemistry, Nankai University, Tianjin 300071, China

[e] Frontier Institute of Science and Technology, and School of Science, Xi'an Jiaotong University, Xi'an 710049, China

[f] Department of Physics, Organic and Carbon Electronics Lab (ORaCEL), North Carolina State University, Raleigh NC 27695, USA

Table of Content

Instruments

^{1}H NMR and ^{13}C NMR spectra were recorded using a Bruker 400-MHz spectrometer in chloroform-d ($CDCl_3$) or 1,1,2,2-tetrachloroethane-d_2 ($C_2D_2Cl_4$) at 25 ^{o}C with tetramethylsilane (TMS) as internal reference. Elemental analysis was conducted on a FlashEA1112 elemental analyzer. Matrix-assisted laser desorption ionization time-of-flight (MALDI-TOF) mass spectra were measured by a Bruker/AutoflexIII Smartbean MALDI mass spectrometer with 2-[(2E)-3-(4-t-buthylphenyl)-2-methylprop-2-enylidene]malononitrile (DCTB) as the matrix in a reflection mode. Thermogravimetric analysis (TGA) was carried out on a TA Q50 thermogravimetric analyzer with the heating rate of 10 ^{o}C min^{-1} at a nitrogen flow. Differential scanning calorimetry (DSC) was conducted on a TA Q2000 instrument with a heating/cooling rate of 10 ^{o}C min^{-1} under nitrogen. UV-vis-NIR absorption spectra (Fig. 2 and S28) were obtained on a Shimadzu UV3600-plus spectrometer. Solution spectra were measured in CF with a concentration of 1×10^{-5} mol L^{-1} and films were prepared by spin-casting with CF as solvent. The optical bandgap was calculated according to absorption onset of films ($E_g^{opt} = 1240/\lambda_{onset}$ eV). Cyclic voltammetry (CV) measurements were carried out on a CHI660a electrochemical workstation at a scan rate of 100 mV s^{-1}. A glassy carbon with 1 cm diameter, a Pt wire and a saturated calomel electrode (SCE) were used as working electrode, counter electrode and reference electrode, respectively. NBu_4PF_6 (0.1 M) in anhydrous acetonitrile was used as electrolyte. The potential was calibrated by ferrocene/ferrocenium (Fc/Fc^{+}). The HOMO and LUMO energy levels were estimated by the equations: $E_{HOMO} = -(4.80 + E_{onset}^{ox})$ eV and $E_{LUMO} = -(4.80+E_{onset}^{re})$ eV,

in which E_{onset}^{ox} and E_{onset}^{re} are oxidation and reduction onsets versus the half potential of Fc/Fc^+, respectively. Density functional theory (DFT) calculations were conducted by Gaussian 09 with a hybrid B3LYP correlation functional and 6-31G (d) basis set and the alkyl side chain was simplified as methyl group. The two-dimensional grazing incidence wide angle X-ray scattering (2D GIWAXS) was measured at the Beamline 7.3.3, Advanced Light Source (ALS), Lawrence Berkeley National Lab. In plane and out of plane GIWAXS of the thin films were measured by a Rigaku Smart Lab with Cu K_α source (λ = 1.54056 Å) in air. Atomic force microscopy (AFM) measurements were performed in tapping mode on a Bruker MultiMode 8 instrument. Film-depth-dependent light absorption spectra (FLAS) (Fig. 7 and S36) were acquired by a home-made setup. During the etching of the films by oxygen plasma (pressure less than 20 Pa), the absorption spectra were in situ monitored by a spectrometer. The FLAS were derived from the in-situ evolution of absorption spectra.

Fabrication and characterization of OSC devices

OSC devices with a conventional architecture of ITO/PEDOT:PSS (30 nm)/active layer/PDINO (10 nm)/Al (100 nm) were fabricated with CF or THF as solvent. ITO was cleaned ultrasonically with soap deionized water, deionized water, acetone and isopropanol for 10 min, successively. The dried ITO was treated with UV-ozone for 25 min. Then a solution of PEDOT:PSS (Baytron PVP Al4083) was spin-coated on the surface at a spinning rate of 4500 r.p.m. for 20 s. After baking at 140 ^oC for 20 min, the substrates were transferred into glovebox under N_2 atmosphere. A CF or THF solution

(totally 17.5mg/mL) of donor:acceptor blend was subsequently spin-coated on the PEDOT:PSS layer to form an active layer. Then the substrates were placed in a glass petri dish containing different solvents (Tol or CF) for solvent vapor annealing (SVA) for various durations. And the substrates were removed. Then, PDINO in methanol solution was deposited on the active layer to give an interfacial layer. Aluminum top electrode (ca. 100 nm) was subsequently deposited on the PDINO layer under high vacuum (< 1.5×10^{-4} Pa). The active area of devices is 4 mm^2, as defined by masks for the solar cell devices. Keithley 2400 source meter was used to measure *J-V* curves under 100 mW cm^{-2} AM 1.5G simulated solar light illumination provided by a Solar Simulator (SS-F5-3A, Enli Technology Co. Ltd) calibrated with a standard photovoltaic cell equipped with a KG5 filter in a glove box. The EQE curves were recorded by the integrated quantum efficiency measurement system QE-R (Enli Technology Co. Ltd., Taiwan), which was calibrated with a crystal silicon photovoltaic cell ahead of the measurement. The active layer thickness was measured using a Dektak150 profilometer.

SCLC measurement

The hole/electron mobility was measured using the space charge limited current (SCLC) method. Hole-only and electron-only devices were fabricated with architecture of ITO/PEDOT:PSS (30 nm)/active layer (120 nm)/Au (100 nm) and ITO/ZnO (30 nm)/active layer (120 nm)/Al (100 nm), respectively. The devices were measured using Keithley 2400 source meter in the dark and the mobilities were obtained by taking

current-voltage curves and fitting the results to a space charge limited form, where the SCLC is described by:

$$J = \frac{9}{8}\varepsilon_0\varepsilon_r\mu\frac{V^2}{L^3}$$

Where J is the current density, L is the thickness of the film, μ is the hole or electron mobility, ε_0 is the permittivity of free space, ε_r is the relative permittivity of the material (assumed to be 3), V (= V_{appl} - V_{bi}) is the internal voltage in the device, where V_{appl} is the applied voltage, V_{bi} is the built-in voltage (0 V), V_{rs} is the voltage drop from the substrate's series resistance (V_{rs} = IR, R is measured to be 10.8 Ω).

Materials and synthesis

All chemical raw materials were purchased from commercial sources and used without further purification. Anhydrous dichloromethane, toluene and triethylamine were distilled before use from Calcium hydride or sodium. Anhydrous chloroform (CF) and tetrahydrofuran (THF) were purchased from Sigma-Aldrich. PDINO were purchased from Derthon Optoelectronic Materials Science Technology Co Ltd. F-2Cl were synthesized according to previous report.[1] Organotin monomers (3,6-bis(5-(2-ethylhexyl)thiophen-2-yl)thieno[3,2-b]thiophene-2,5-diyl)bis(trimethylstannane) (**1a**), (3,6-bis(2-ethylhexyl)thieno[3,2-b]thiophene-2,5-diyl)bis(trimethylstannane) (**1b**), (3,6-bis((2-ethylhexyl)oxy)thieno[3,2-b]thiophene-2,5-diyl)bis(trimethylstannane) (**1c**) and 2,5-bis(trimethylstannyl)thieno[3,2-b]thiophene (**1d**) were synthesized according to the literature.[2-4]

6,6'-(3,6-bis(5-(2-ethylhexyl)thiophen-2-yl)thieno[3,2-b]thiophene-2,5-diyl)bis(4,8-bis(5-(2-ethylhexyl)thiophen-2-yl)benzo[1,2-b:4,5-b']dithiophene-2-carbaldehyde) (**3a**). To a reaction tube were added compound **1a** (100 mg, 0.117 mmol), **2** (176 mg, 0.257 mmol), $Pd(PPh_3)_4$ (6.73 mg, 0.005 mmol) and anhydrous toluene (1.00 mL) in glove box. The mixture was stirred in a microwave reactor at a dynamic model (170 ^oC, 200 W) for 1 hour. Then the reaction mixture was poured into water and extracted with $CHCl_2$. The combined organic extracts were dried over anhydrous $MgSO_4$. After evaporating the solvent, the residue was purified by column chromatography on silica gel with $CHCl_3$ as eluent to afford the product as a red solid (172 mg, 85%). ^1H NMR ($CDCl_3$, 400 MHz): δ (ppm) = 10.05 (s, 2H), 8.33 (s, 2H), 7.76 (s, 2H), 7.29 (d, 2H), 7.23 (d, 2H), 7.15 (d, 2H), 6.90 (d, 2H), 6.85 (d, 2H), 6.75 (d, 2H), 2.87-2.83 (m, 8H), 2.77 (d, 4H), 1.75-1.65 (m, 4H), 1.57-1.63 (m, 2H), 1.48-1.20 (48H), 1.00-0.80 (m, 36H). ^{13}C NMR (100 MHz, $CDCl_3$): δ (ppm) = 184.68, 146.85, 146.50, 146.42, 143.41, 141.36, 139.85, 139.78, 139.41, 139.37, 135.80, 135.75, 135.51, 134.64, 132.82, 131.80, 128.33, 128.24, 127.95, 126.51, 126.48, 125.72, 125.57, 125.51, 124.64, 123.85, 41.46, 41.26, 34.32, 34.27, 34.14, 32.50, 32.40, 30.16, 29.73, 28.92, 28.84, 25.73, 25.69, 25.48, 23.05, 23.00, 14.20, 14.15, 10.90, 10.78. MS (MALDI-TOF) *m/z*: calcd. for $C_{100}H_{120}O_2S_{12}$: 1737.60; Found. 1738.61. Elemental Anal. Calcd.: C, 69.08; H, 6.96; S, 22.13; Found. C, 69.23; H, 6.85; S, 22.31.

6,6'-(3,6-bis(2-ethylhexyl)thieno[3,2-b]thiophene-2,5-diyl)bis(4,8-bis(5-(2-ethylhexyl)thiophen-2-yl)benzo[1,2-b:4,5-b']dithiophene-2-carbaldehyde) (**3b**). **3b** (112 mg, 82%) was obtained as a red solid from **1b** (60.0 mg, 0.087 mmol) and **2** (131.2

mg, 0.191 mmol) following the procedure for the synthesis of **3a**. ^{1}H NMR ($CDCl_3$, 400 MHz): δ (ppm) = 10.06 (s, 2H), 8.34 (s, 2H), 7.75 (s, 2H), 7.35 (d, 2H), 7.33 (d, 2H), 6.91 (d, 2H), 6.94 (d, 2H), 2.92-2.86 (m, 12H), 1.95-1.92 (m, 2H), 1.72-1.68 (m, 4H), 1.48-1.20 (48H), 1.00-0.80 (m, 36H). ^{13}C NMR (100 MHz, $CDCl_3$): δ (ppm) = 184.70, 146.96, 146.54, 143.31, 141.63, 140.59, 140.34, 139.70, 139.36, 135.95, 135.80, 135.31, 134.64, 133.23, 132.65, 128.38, 128.17, 126.53, 125.80, 125.66, 124.35, 121.98, 41.50, 39.17, 34.30, 34.26, 33.75, 32.81, 32.50, 32.48, 31.94, 30.32, 29.71, 29.34, 28.91, 28.59, 27.22, 26.16, 25.75, 25.68, 23.06, 23.03, 22.71, 14.18, 14.14, 14.06, 10.91, 10.89, 10.86. MS (MALDI-TOF) *m/z*: calcd. for $C_{92}H_{116}O_2S_{10}$: 1572.62; Found. 1573.72. Elemental Anal. Calcd.: C, 70.18; H, 7.43; S, 20.36; Found. C, 70.31; H, 7.29; S, 20.15.

6,6'-(3,6-bis((2-ethylhexyl)oxy)thieno[3,2-b]thiophene-2,5-diyl)bis(4,8-bis(5-(2-ethylhexyl)thiophen-2-yl)benzo[1,2-b:4,5-b']dithiophene-2-carbaldehyde) (**3c**). **3c** (87.2 mg, 75%) was obtained as a dark red solid from **1c** (50.0 mg, 0.072 mmol) and **2** (109.3 mg, 0.159 mmol) following the procedure for the synthesis of **3a**. ^{1}H NMR ($CDCl_3$, 400 MHz): δ (ppm) = 10.01 (s, 2H), 8.30 (s, 2H), 7.74 (s, 2H), 7.35 (d, 2H), 7.30 (d, 2H), 6.93 (d, 2H), 6.91 (d, 2H), 4.39-4.32 (4H), 2.90-2.88 (m, 8H), 1.82-1.67 (m, 6H), 1.55-1.26 (48H), 1.00-0.86 (m, 36H). ^{13}C NMR (100 MHz, $CDCl_3$): δ (ppm) = 184.38, 147.47, 146.60, 146.14, 142.71, 141.65, 139.54, 138.78, 138.30, 136.27, 136.00, 134.90, 134.58, 128.40, 128.19, 126.81, 126.27, 125.60, 125.54, 123.41, 118.96, 118.20, 74.63, 41.46, 41.44, 40.20, 34.34, 34.30, 32.56, 32.51, 30.21, 29.73, 29.15, 28.95, 28.94, 25.71, 25.68, 23.69, 23.08, 23.04, 14.21, 14.19, 11.20, 10.93,

10.88. MS (MALDI-TOF) *m/z*: calcd. for $C_{92}H_{116}O_4S_{10}$: 1604.61; Found. 1605.85. Elemental Anal. Calcd.: C, 68.78; H, 7.28; S, 19.96; Found. C, 68.94; H, 7.39; S, 19.75.

6,6'-(thieno[3,2-b]thiophene-2,5-diyl)bis(4,8-bis(5-(2-ethylhexyl)thiophen-2-yl)benzo[1,2-b:4,5-b']dithiophene-2-carbaldehyde) (**3d**). **3d** (150 mg, 87%) was obtained as a red solid from **1d** (60 mg, 0.128 mmol) and **2** (194 mg, 0.283 mmol) following the procedure for the synthesis of **3a**. ^{1}H NMR ($C_2D_2Cl_4$, 400 MHz): δ (ppm) = 9.96 (s, 2H), 8.32 (s, 2H), 7.68 (s, 2H), 7.43 (s, 2H), 7.41 (d, 2H), 7.38 (d, 2H), 7.05 (d, 2H), 7.03 (d, 2H), 3.02-2.97 (m, 8H), 1.87-1.78 (m, 4H), 1.60-1.40 (16H), 1.12-1.00 (m, 12H). ^{13}C NMR (100 MHz, $C_2D_2Cl_4$): δ (ppm) =184.40, 147.01, 146.58, 142.84, 141.49, 140.02, 139.96, 139.65, 139.50, 138.39, 135.85, 135.67, 135.23, 134.66, 128.72, 128.53, 126.38, 125.99, 125.86, 123.98, 119.00, 117.95, 41.55, 34.47, 32.72, 32.66, 29.13, 29.11, 25.96, 23.33, 23.32, 14.57, 14.55, 11.24, 11.21. MS (MALDI-TOF) *m/z*: calcd. for $C_{76}H_{84}O_2S_{10}$: 1348.37; Found. 1349.60. Elemental Anal. Calcd.: C, 67.61; H, 6.27; S, 23.75; Found. C, 67.80; H, 6.09; S, 23.61.

DRTT-T. A solution of compound **3a** (100 mg, 0.058 mmol) and 3-ethyl-2-thioxothiazolidin-4-one (93 mg, 0.580 mmol) in dry $CHCl_3$ (8 mL) was degassed twice with argon followed by the addition of a few drops of triethylamine. Then the reaction mixture was stirred at 70 °C for 8 hours. The solvent was removed under reduced pressure and the residues were purified by column chromatography on silica gel with $CHCl_3$ as eluent and Concentrated to a saturated solution then added dropwise in methanol for precipitation. The solid was collected by filtration to afford the product as a dark red solid (100 mg, 86%). ^{1}H NMR ($CDCl_3$, 400 MHz): δ (ppm) = 7.96 (s, 2H),

7.91 (s, 2H), 7.74 (s, 2H), 7.27 (d, 2H), 7.23 (s, 2H), 7.13 (d, 2H), 6.88 (m, 4H), 6.74 (m, 2H), 4.21-4.16 (m, 4H), 2.87-2.85 (m, 8H), 2.78-2.76 (m, 4H), 1.72-1.68 (m, 4H), 1.62-1.56 (m, 2H), 1.48-1.20 (54H), 0.80-1.00 (m, 36H). ^{13}C NMR (100 MHz, $CDCl_3$): δ (ppm) = 192.34, 167.14, 146.63, 146.44, 146.35, 141.50, 139.93, 139.76, 138.76, 138.19, 138.01, 136.05, 135.97, 133.05, 131.84, 131.75, 128.21, 128.18, 127.97, 126.20, 125.95, 125.64, 125.47, 125.20, 124.03, 123.69, 123.60, 41.46, 41.24, 39.95, 34.40, 34.26, 34.16, 32.55, 32.50, 32.40, 29.73, 28.95, 28.92, 28.84, 25.76, 25.70, 25.46, 23.10, 23.07, 23.02, 14.23, 14.17, 12.31, 10.98, 10.91, 10.77. MS (MALDI-TOF) *m/z*: calcd. for $C_{110}H_{130}N_2O_2S_{16}$: 2023.57; Found. 2024.78. Elemental Anal. Calcd.: C, 65.24; H, 6.47; N, 1.38; S, 25.33; Found. C, 65.39; H, 6.27; N, 1.49; S, 25.42.

DRTT-R. DRTT-R (134 mg, 88%) was obtained as a dark red solid from **3b** (130 mg, 0.830 mmol) and 3-ethyl-2-thioxothiazolidin-4-one (133 mg, 0.830 mmol) following the procedure for the synthesis of DRTT-T. ^{1}H NMR ($CDCl_3$, 400 MHz): δ (ppm) = 7.96 (s, 2H), 7.91 (s, 2H), 7.72 (s, 2H), 7.34 (d, 4H), 6.95 (d, 2H), 6.93 (d, 2H), 4.20-4.15 (m, 4H), 2.92-2.89 (m, 12H), 1.94-1.92 (m, 2H), 1.74-1.70 (m, 4H), 1.46-1.20 (54H), 1.00-0.91 (m, 24H), 0.86-0.79 (m, 12H). ^{13}C NMR (100 MHz, $CDCl_3$): δ (ppm) = 192.33, 167.13, 146.73, 146.56, 146.47, 141.78, 140.54, 139.72, 139.34, 139.16, 138.48, 137.87, 136.13, 135.79, 132.95, 132.85, 131.75, 128.27, 128.10, 125.94, 125.73, 125.17, 123.69, 123.51, 121.61, 41.49, 39.93, 39.15, 34.35, 34.30, 33.89, 32.79, 32.65, 32.58, 32.51, 29.73, 28.96, 28.92, 28.58, 26.18, 25.83, 25.73, 23.09, 14.23, 14.09, 12.30, 11.07, 10.98, 10.92, 10.88. MS (MALDI-TOF) *m/z*: calcd. for

$C_{102}H_{126}N_2O_2S_{14}$: 1859.59; Found. 1860.78. Elemental Anal. Calcd.: C, 65.83; H, 6.82; N, 1.51; S, 24.12; Found. C, 65.99; H, 6.63; N, 1.67; S, 24.02.

DRTT-OR. DRTT-OR (52 mg, 89%) was obtained as a dark red solid from **3c** (50 mg, 0.031 mmol) and 3-ethyl-2-thioxothiazolidin-4-one (50 mg, 0.310 mmol) following the procedure for the synthesis of DRTT-T. ^{1}H NMR ($CDCl_3$, 400 MHz): δ (ppm) = 7.85 (s, 2H), 7.75 (s, 2H), 7.55 (s, 2H), 7.34 (d, 2H), 7.33 (d, 2H), 6.94 (d, 2H), 6.91 (d, 2H), 4.30 (s, 4H), 4.10-4.05 (m, 4H), 2.94-2.90 (m, 8H), 1.80-1.72 (m, 6H), 1.56-1.32 (48H), 1.28-1.20 (m, 6H), 1.10-0.92 (m, 36H). ^{13}C NMR (100 MHz, $CDCl_3$): δ (ppm) = 192.14, 166.89, 147.02, 146.23, 145.85, 141.71, 138.73, 138.02, 137.43, 136.94, 136.45, 135.13, 131.90, 128.37, 128.19, 126.37, 125.85, 125.51, 125.43, 124.76, 122.50, 118.88, 117.57, 77.35, 77.03, 76.71, 74.50, 41.42, 41.40, 40.11, 39.66, 34.44, 34.34, 32.67, 32.55, 30.07, 29.73, 29.12, 29.00, 28.95, 25.76, 25.61, 23.55, 23.15, 23.14, 23.08, 14.28, 14.25, 14.24, 12.27, 11.16, 11.04, 10.85. MS (MALDI-TOF) *m/z*: calcd. for $C_{102}H_{126}N_2O_4S_{14}$: 1891.58; Found. 1892.65. Elemental Anal. Calcd.: C, 64.72; H, 6.71; N, 1.48; S, 23.71; Found. C, 64.56; H, 6.92; N, 1.59; S, 23.85.

DRTT. DRTT (48 mg, 80%) was obtained as a dark purple solid from **3d** (50 mg, 0.037 mmol) and 3-ethyl-2-thioxothiazolidin-4-one (60 mg, 0.370 mmol) following the procedure for the synthesis of DRTT-T. ^{1}H NMR ($CDCl_3$, 400 MHz): δ (ppm) = 7.50 (s, 2H), 7.34 (s, 2H), 7.15 (s, 4H), 7.10 (d, 2H), 6.91 (d, 4H), 6.73 (d, 2H), 3.83-3.81 (m, 4H), 2.96-2.94 (m, 8H), 1.85-1.75 (m, 4H), 1.60-1.40 (m, 32H), 1.09-1.01 (30H). ^{13}C NMR (100 MHz, $CDCl_3$): δ (ppm) = 191.48, 166.33, 146.19, 145.75, 141.35, 138.96, 138.72, 138.45, 137.86, 137.74, 136.86, 136.30, 136.03, 135.18, 131.25,

128.23, 125.36, 124.99, 124.19, 122.72, 122.20, 117.99, 116.89, 41.37, 41.33, 39.28, 34.43, 32.74, 32.64, 29.70, 29.06, 28.99, 25.85, 25.73, 23.27, 23.23, 14.42, 14.35, 12.12, 11.11, 10.92. MS (MALDI-TOF) *m/z*: calcd. for $C_{86}H_{94}N_2O_2S_{14}$: 1634.34; Found. 1635.22. Elemental Anal. Calcd.: C, 63.12; H, 5.79; N, 1.71; S, 27.43; Found. C, 62.99; H, 5.60; N, 1.89; S, 27.65.

Supplementary data

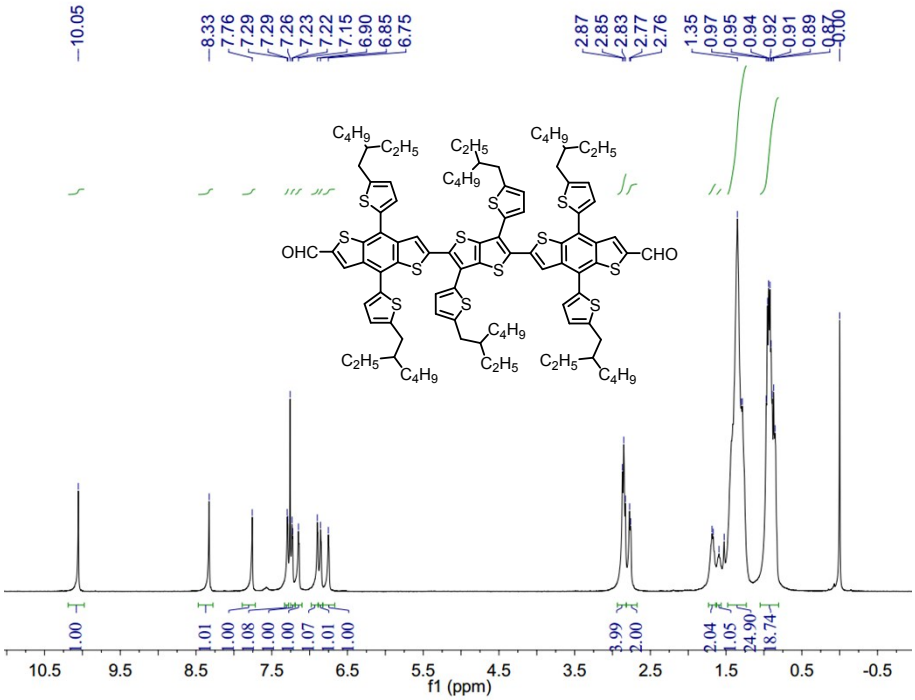

Fig. S1 ^{1}H NMR spectrum of compound **3a**.

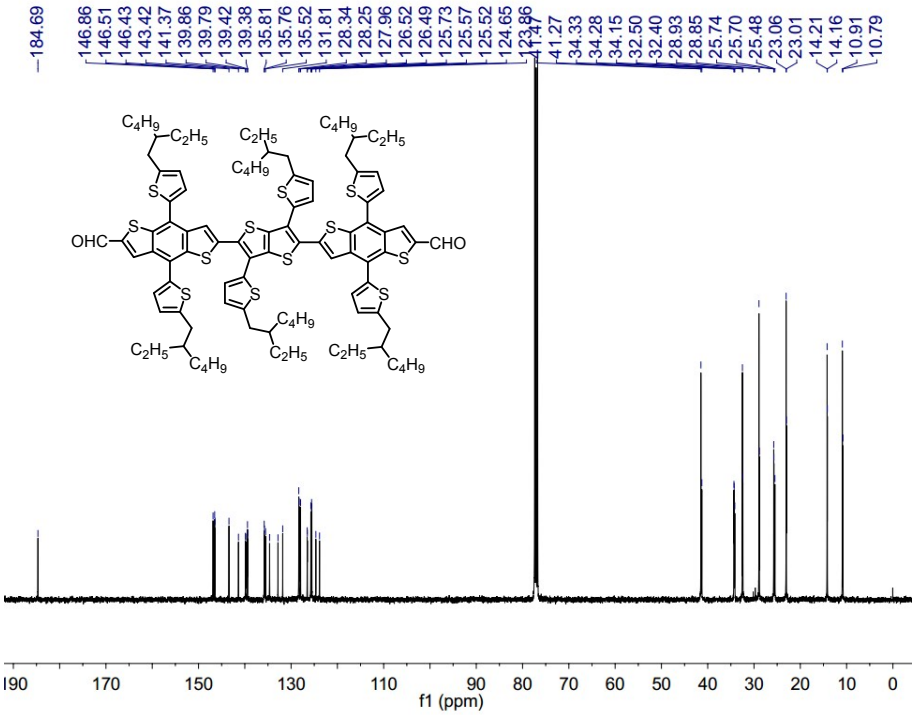

Fig. S2 ^{13}C NMR spectrum of compound **3a**.

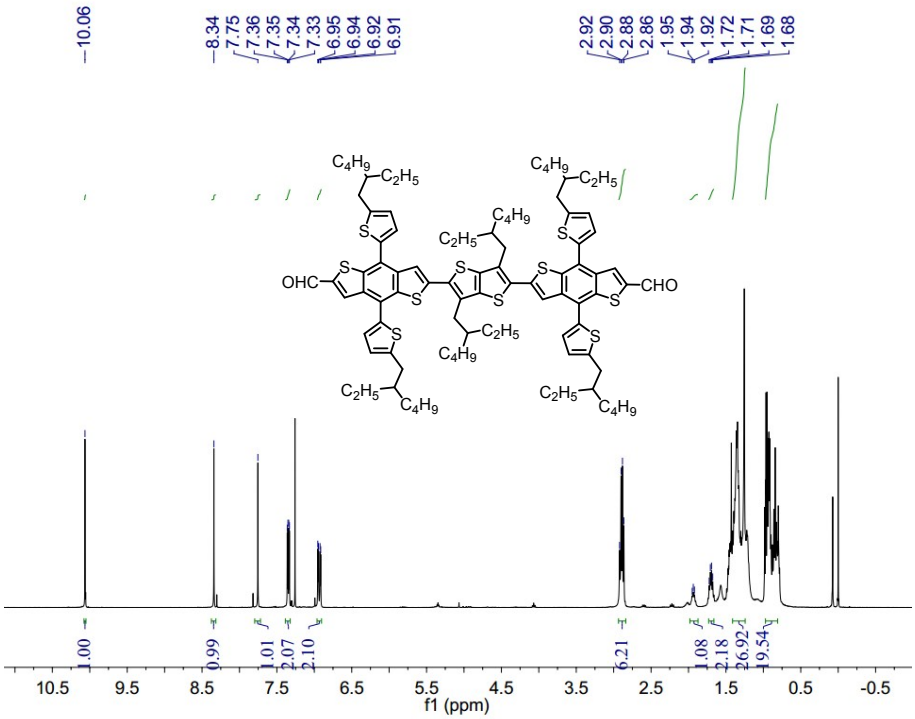

Fig. S3 ^{1}H NMR spectrum of compound **3b**.

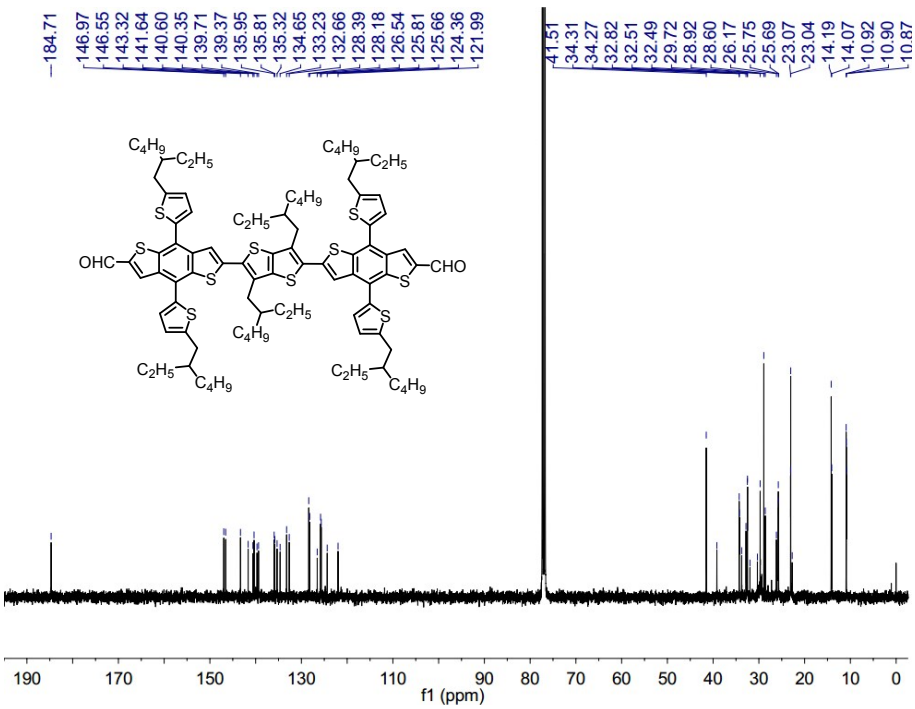

Fig. S4 ^{13}C NMR spectrum of compound **3b**.

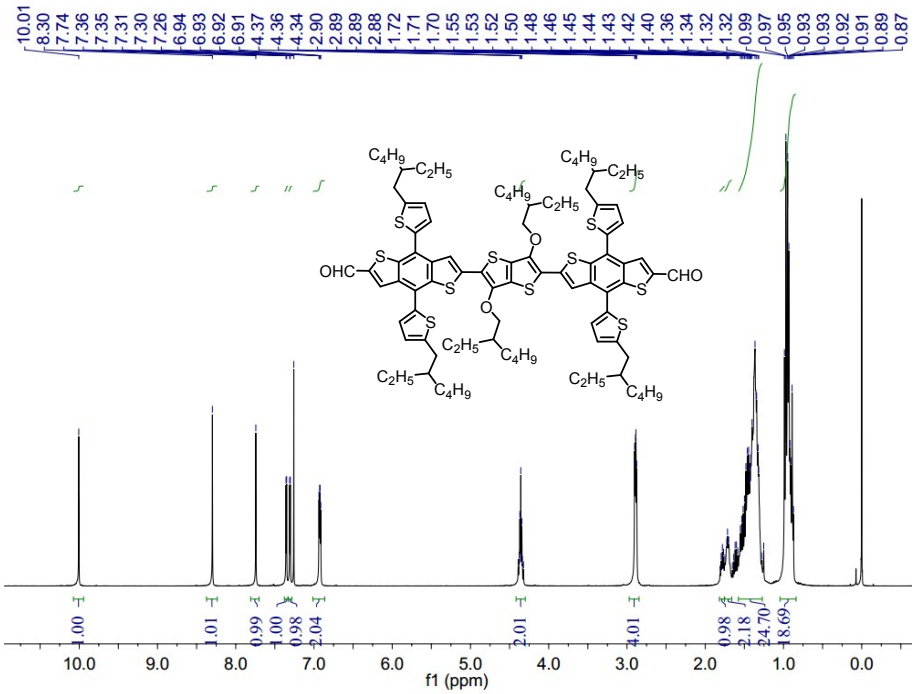

Fig. S5 ^{1}H NMR spectrum of compound **3c**.

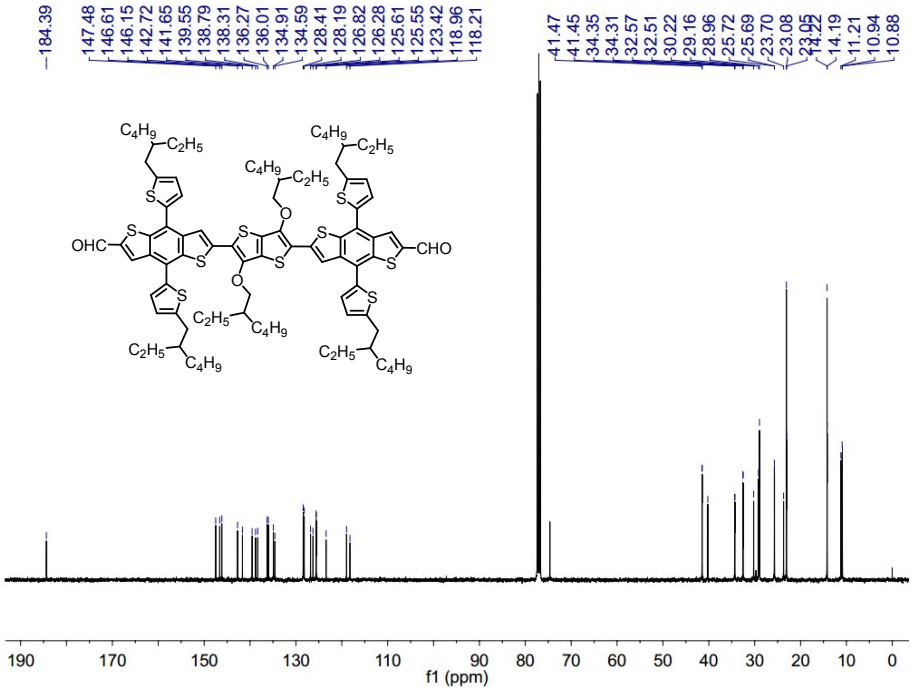

Fig. S6 ^{13}C NMR spectrum of compound **3c**.

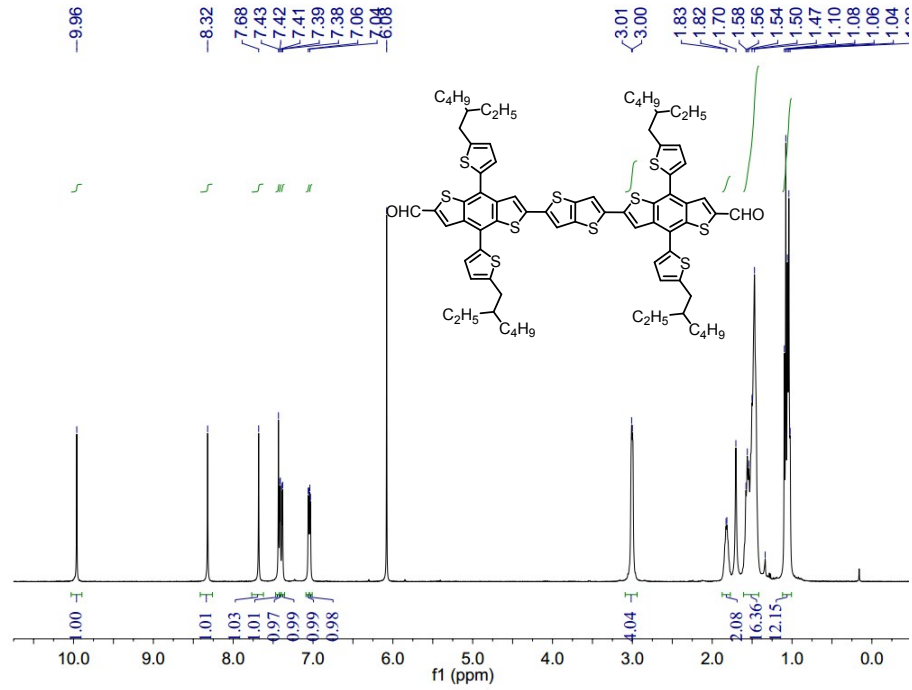

Fig. S7 ^{1}H NMR spectrum of compound **3d**.

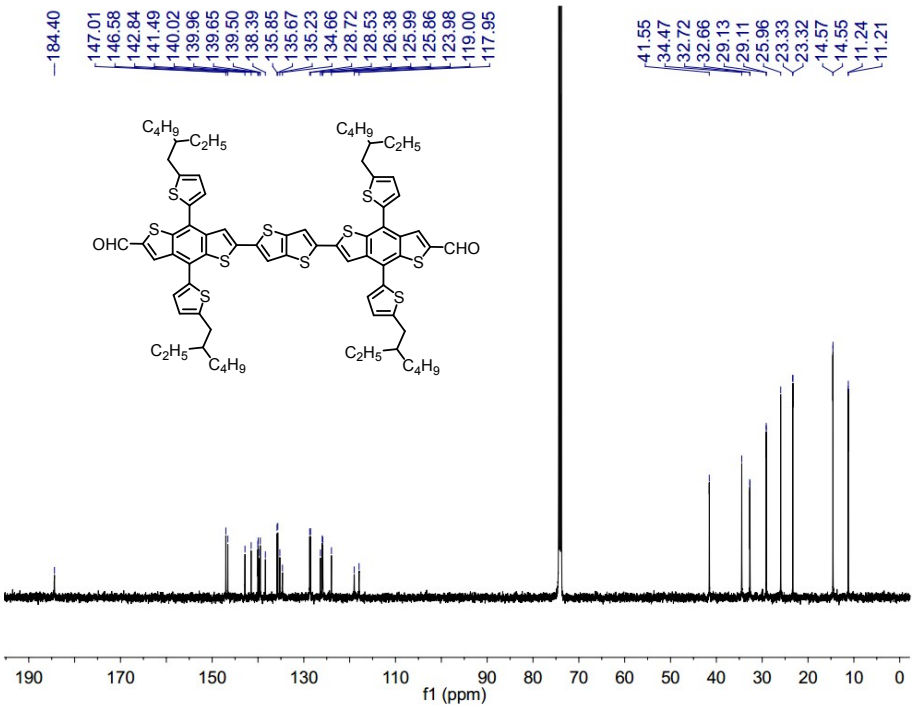

Fig. S8 ^{13}C NMR spectrum of compound **3d**.

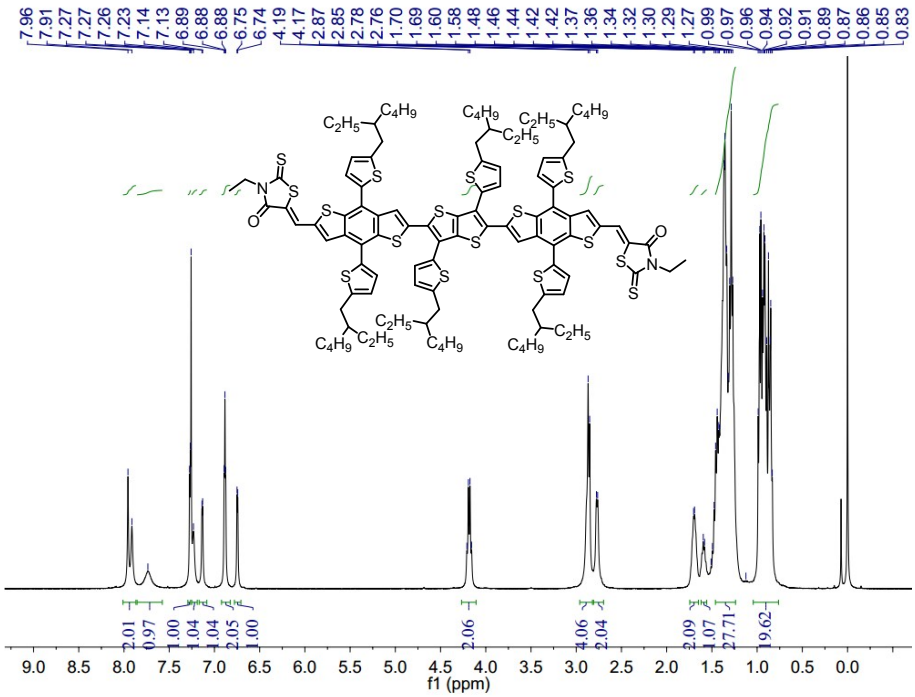

Fig. S9 ^{1}H NMR spectrum of DRTT-T.

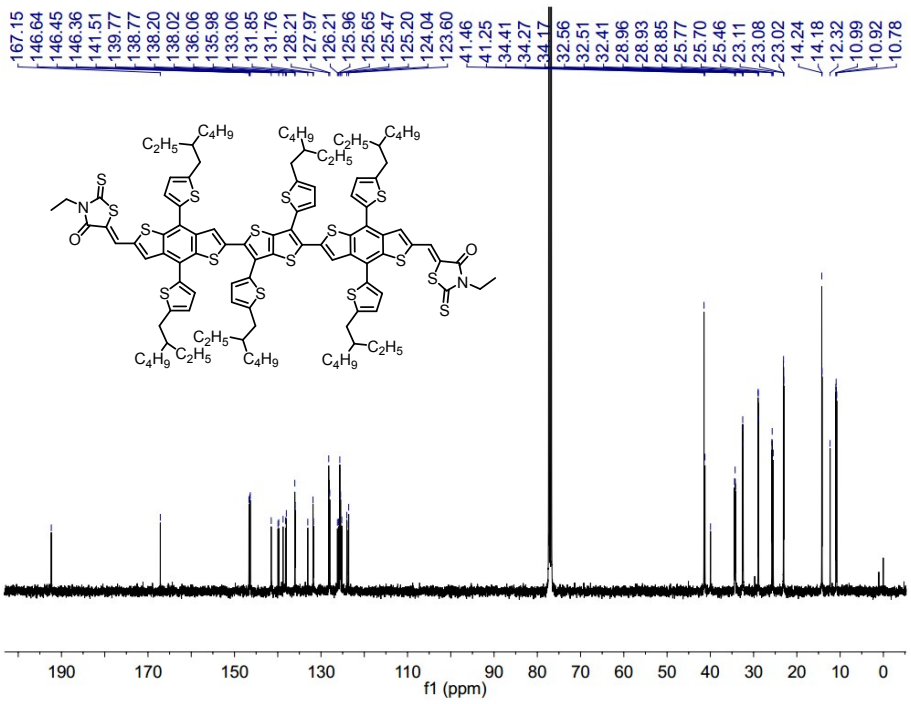

Fig. S10 ^{13}C NMR spectrum of DRTT-T.

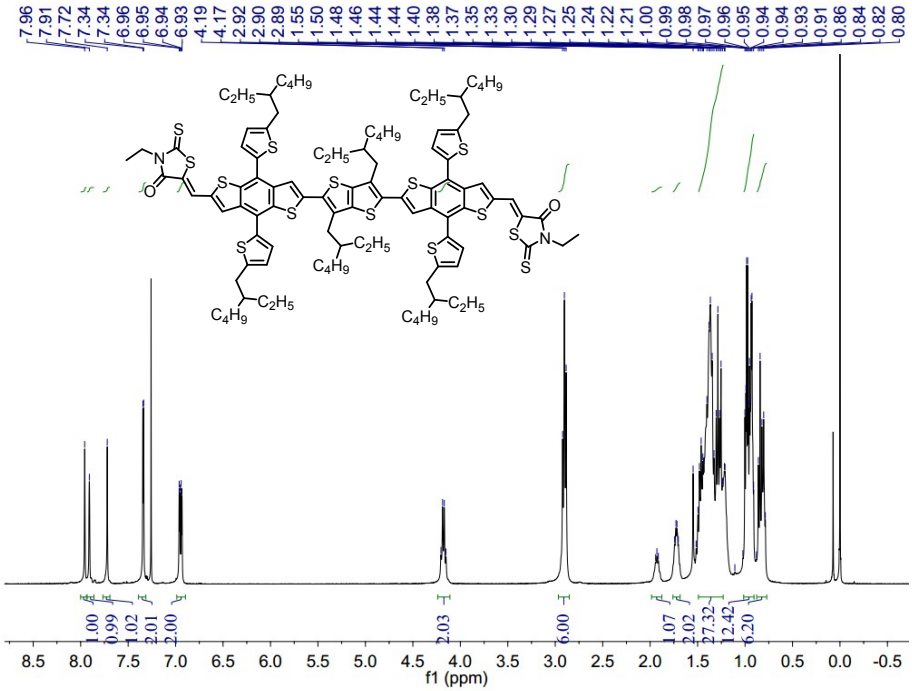

Fig. S11 ^{1}H NMR spectrum of DRTT-R.

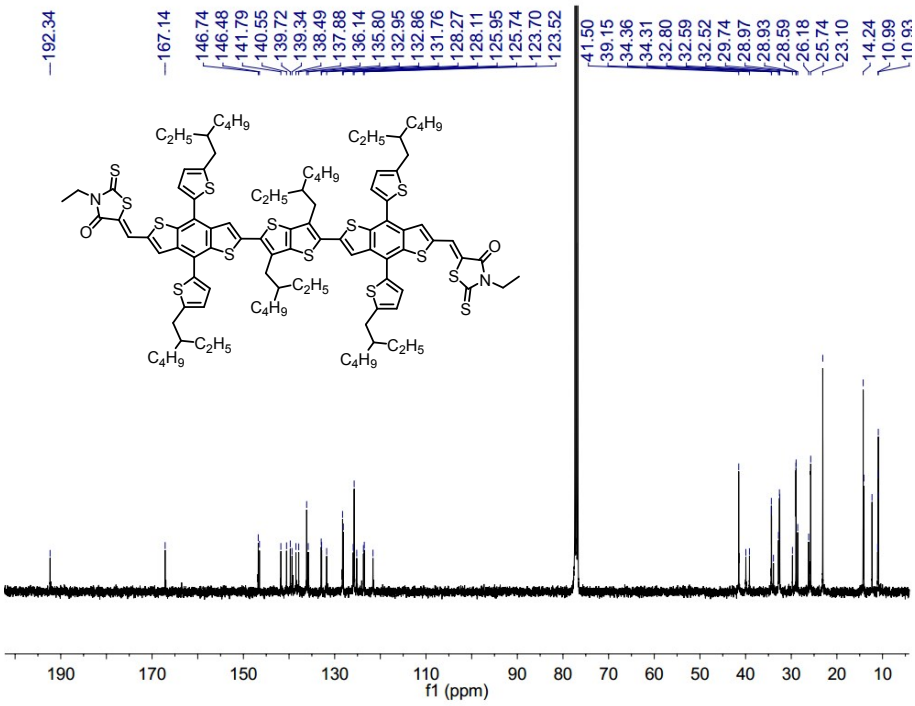

Fig. S12 ^{13}C NMR spectrum of DRTT-R.

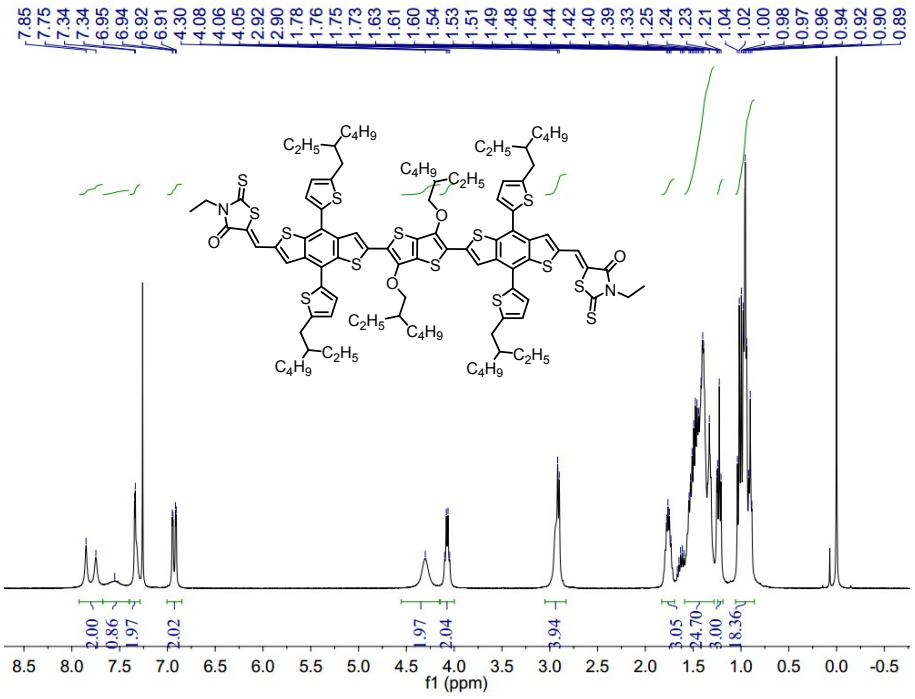

Fig. S13 ^{1}H NMR spectrum of DRTT-OR.

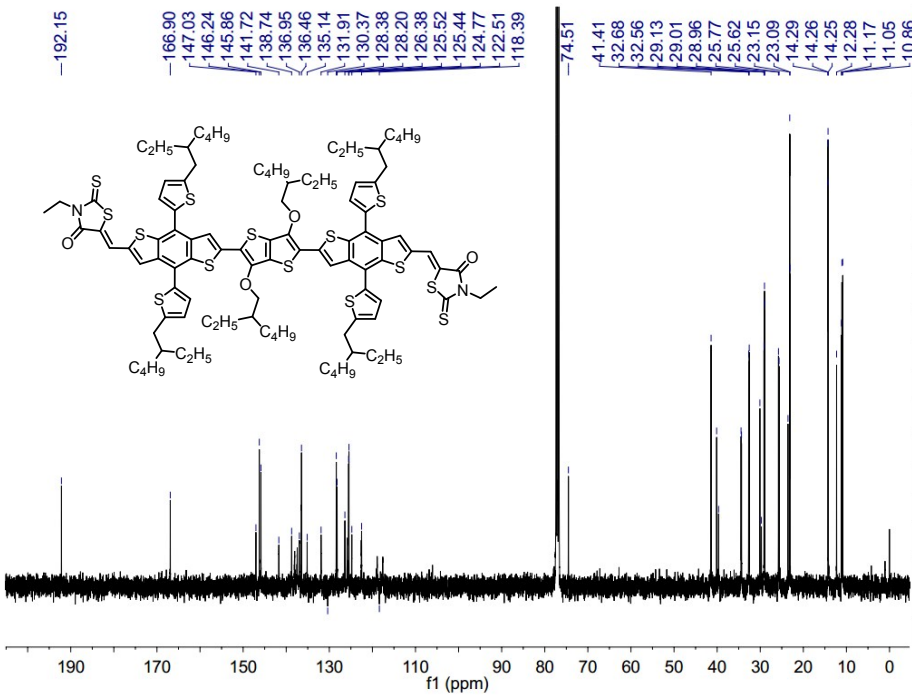

Fig. S14 ^{13}C NMR spectrum of DRTT-OR.

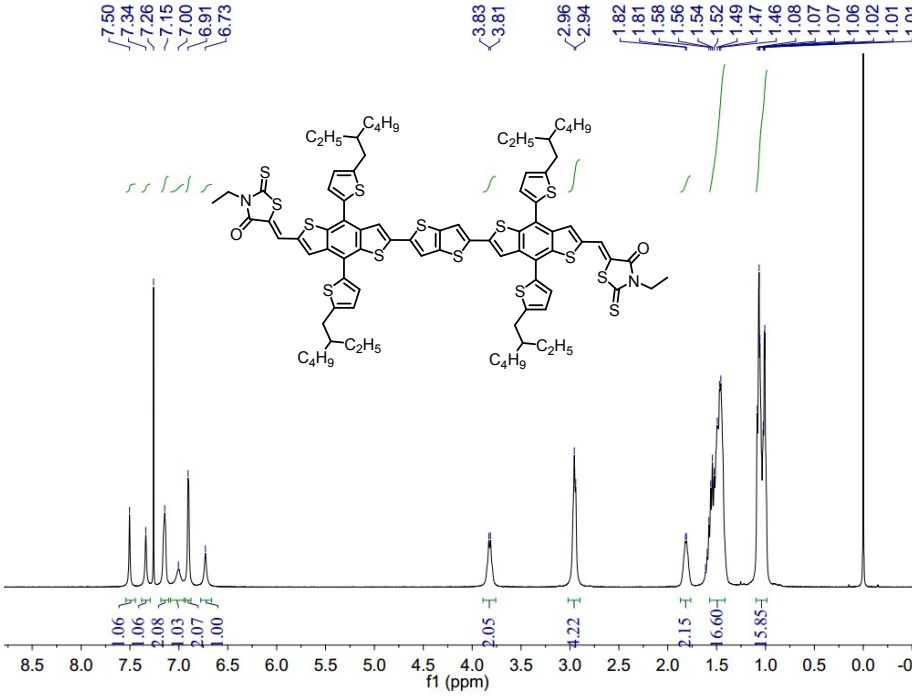

Fig. S15 ^{1}H NMR spectrum of DRTT.

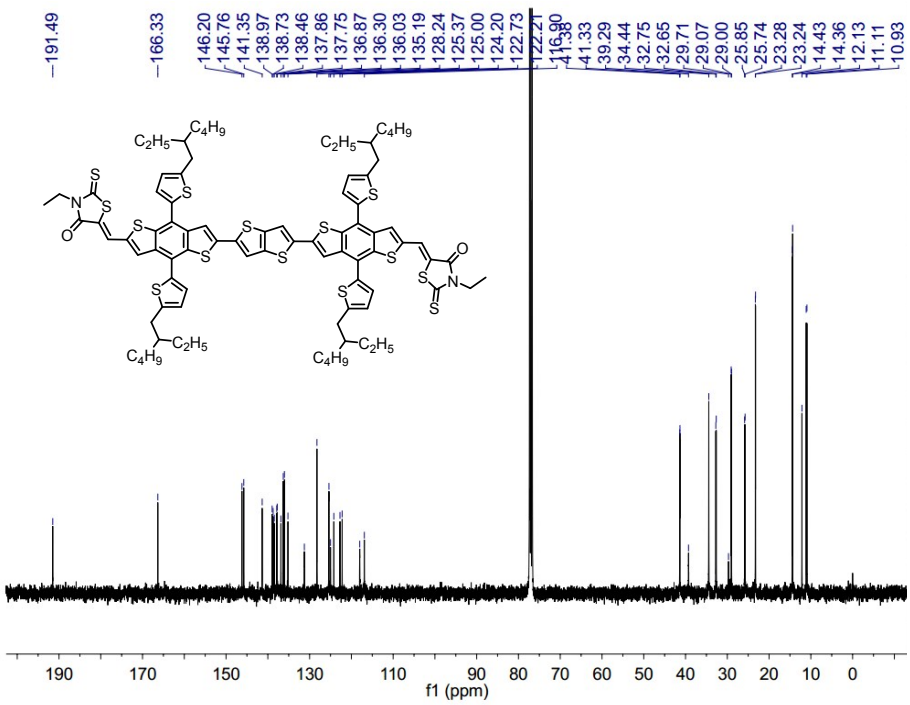

Fig. S16 ^{13}C NMR spectrum of DRTT.

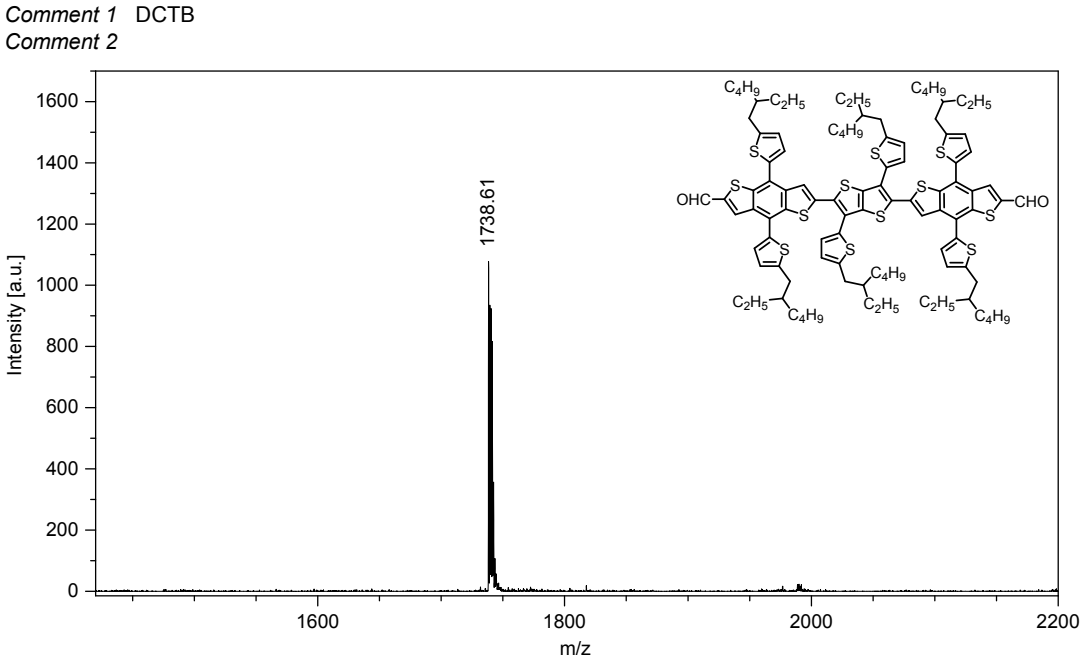

Fig. S17 The MALDI-TOF mass spectrum of compound **3a**.

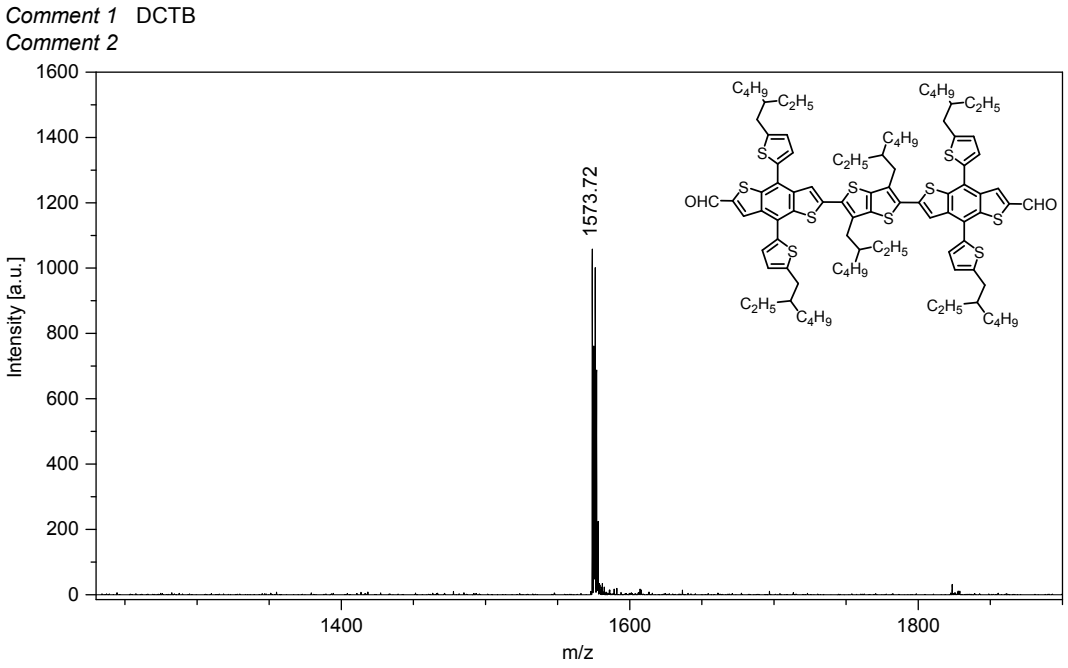

Fig. S18 The MALDI-TOF mass spectrum of compound **3b**.

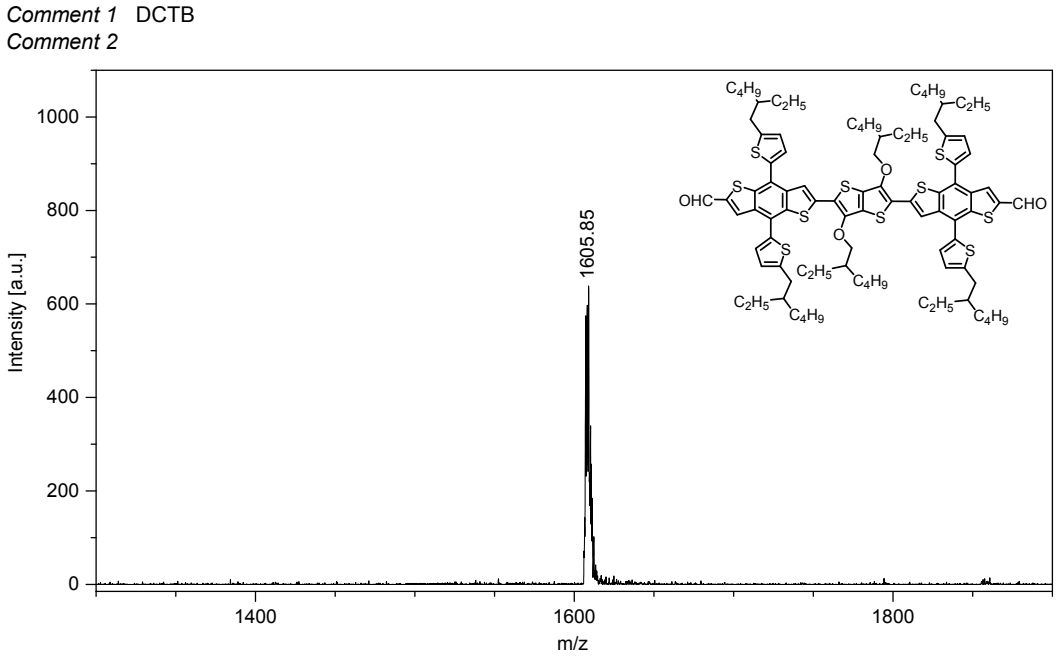

Fig. S19 The MALDI-TOF mass spectrum of compound **3c**.

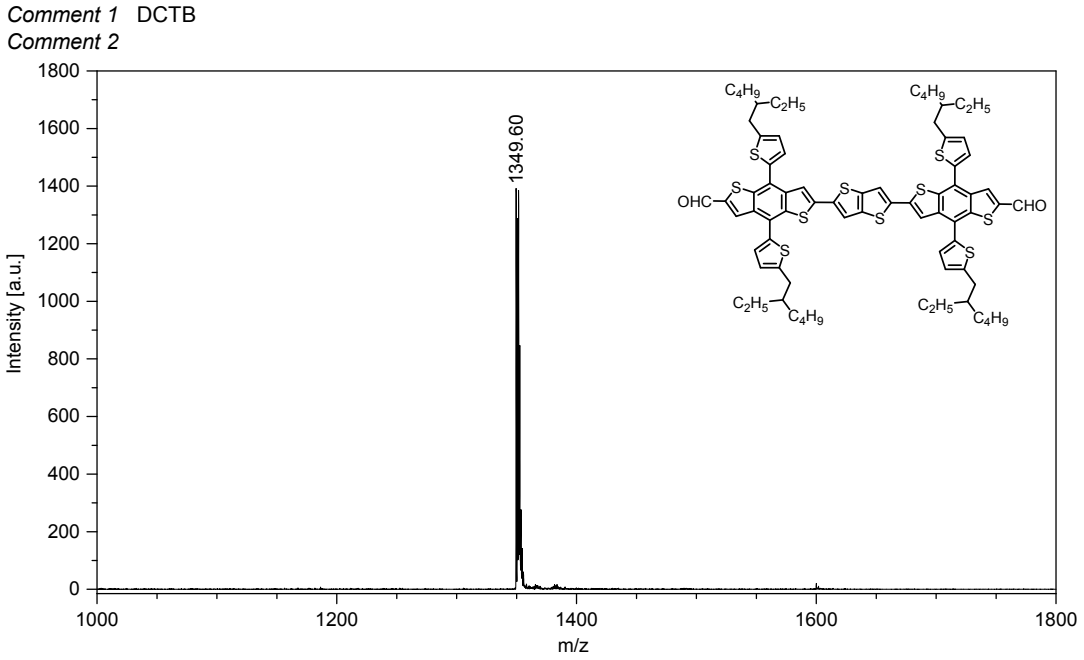

Fig. S20 The MALDI-TOF mass spectrum of compound **3d**.

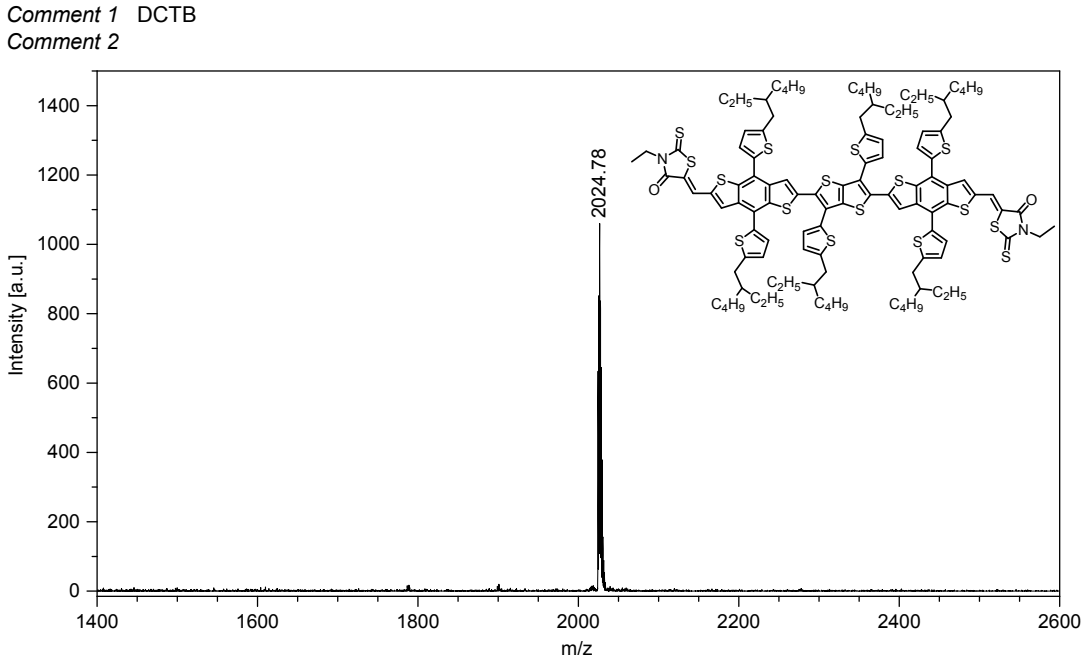

Fig. S21 The MALDI-TOF mass spectrum of DRTT-T.

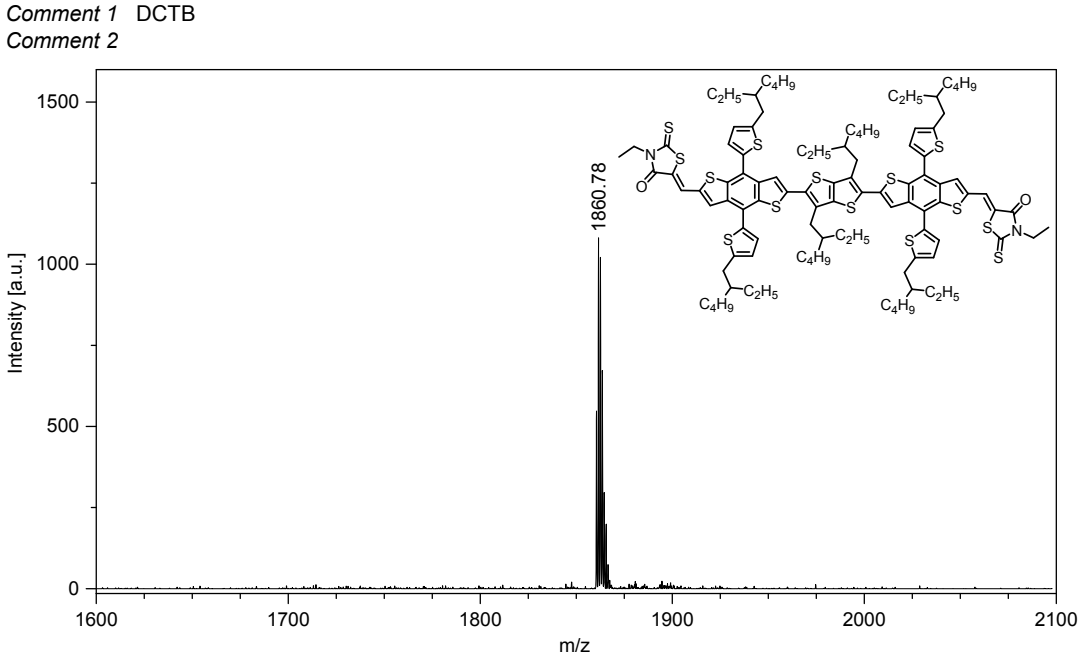

Fig. S22 The MALDI-TOF mass spectrum of DRTT-R.

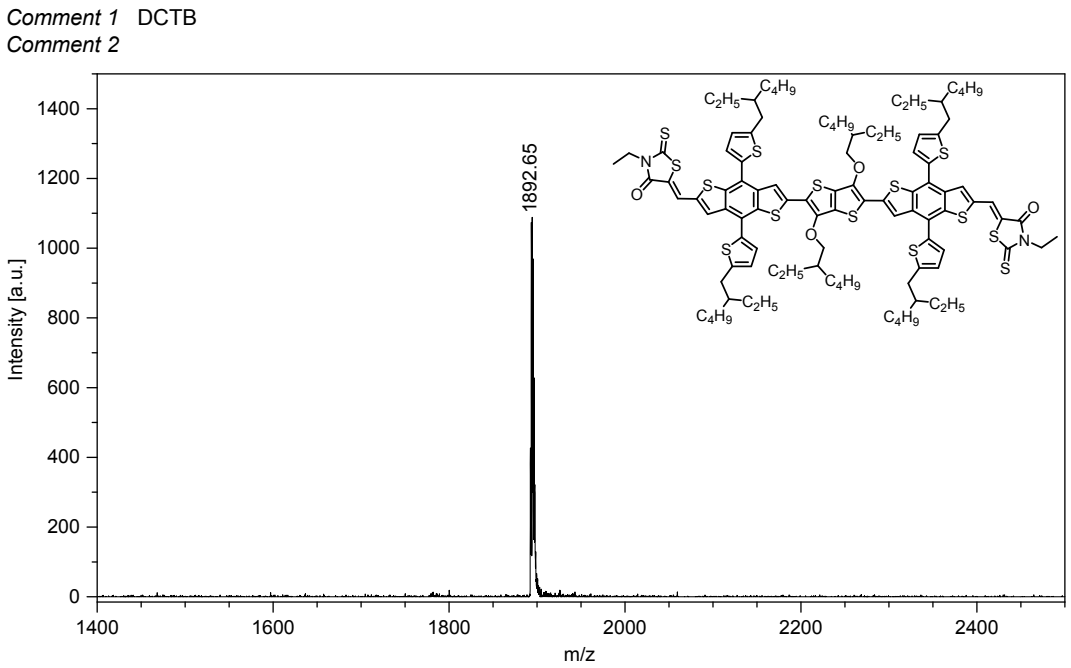

Fig. S23 The MALDI-TOF mass spectrum of DRTT-OR.

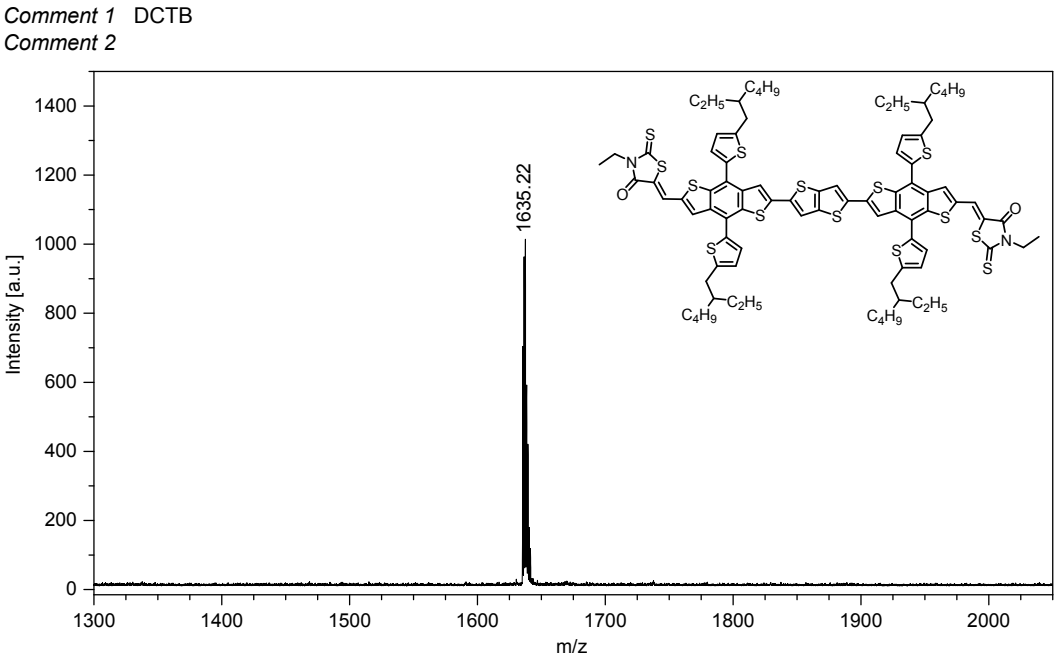

Fig. S24 The MALDI-TOF mass spectrum of DRTT.

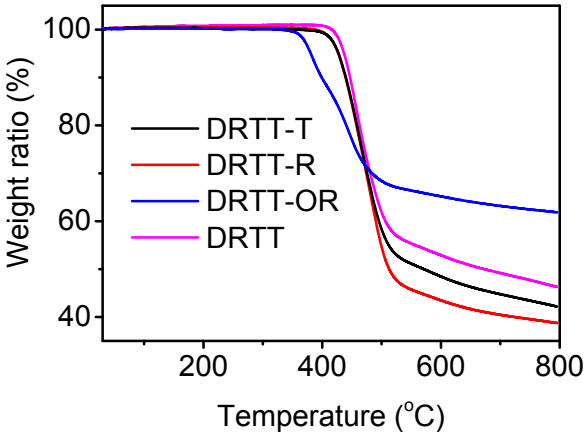

Fig. S25 TGA curves of DRTT-T, DRTT-R, DRTT-OR and DRTT in nitrogen with a heating rate of 10 °C/min.

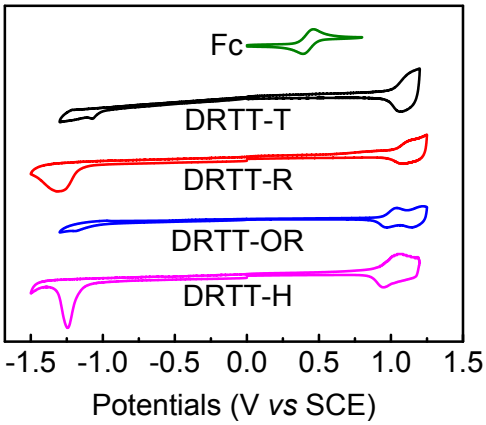

Fig. S26 Thin film cyclic voltammograms (CV) of DRTT-T, DRTT-R, DRTT-OR and DRTT.

Table S1 Out-of-plane XRD data of DRTT-T, DRTT-R, DRTT-OR and DRTT neat films without and with SVA using CF for 80 s.

Out-of-plane	(100) 2θ	(100) *d*-spacing (Å)	(100) FWHM Δθ	(100) Crystal size	(010) 2θ	(010) *d*-spacing (Å)	(010) FWHM Δθ	010) Crystal size
DRTT-T As cast	4.50	19.62	2.54	36.21	N/A	N/A	N/A	N/A
DRTT-T SVA	4.55	19.41	0.83	106.49	23.75	3.74	2.21	40.84
DRTT-R As cast	4.70	18.79	1.04	85.99	N/A	N/A	N/A	N/A
DRTT-R SVA	4.85	18.21	0.95	93.05	23.30	3.79	2.36	35.22
DRTT-OR As cast	4.65	18.99	0.89	99.31	N/A	N/A	N/A	N/A
DRTT-OR SVA	4.70	18.79	0.89	99.32	N/A	N/A	N/A	N/A
DRTT As cast	5.50	16.06	1.65	53.59	N/A	-N/A	N/A	N/A
DRTT SVA	5.50	16.06	1.64	53.91	N/A	N/A	N/A	N/A

[a] N/A denotes not available.

Table S2 In-plane XRD data of DRTT-T, DRTT-R, DRTT-OR and DRTT neat films without and with SVA using CF for 80 s.

In-plane	(100) 2θ	(100) *d*-spacing （Å）	(100) FWHM Δθ	(100) Crystal size	(010) 2θ	(010) *d*-spacing （Å）	(010) FWHM Δθ	(010) Crystal size
DRTT-T As cast	N/A	N/A	N/A	N/A	N/A	N/A	N/A	N/A
DRTT-T SVA	4.26	20.77	0.77	113.30	23.70	3.75	2.87	34.67
DRTT-R As cast	N/A	N/A	N/A	N/A	N/A	N/A	N/A	N/A
DRTT-R SVA	4.45	19.84	0.90	94.02	23.55	3.77	3.18	25.08
DRTT-OR As cast	N/A	N/A	N/A	N/A	23.65	3.77	1.48	62.24
DRTT-OR SVA	N/A	N/A	N/A	N/A	23.66	3.77	1.19	71.62
DRTT As cast	N/A	N/A	N/A	N/A	24.00	3.70	2.65	34.87
DRTT SVA	N/A	N/A	-N/A	N/A	24.30	3.66	2.64	35.01

[a] N/A denotes not available.

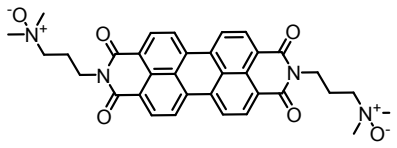

Fig. S27 Chemical structure of PDINO.

Table S3 The detailed photovoltaic performance of OSCs based on DRTT-R:F-2Cl with different D:A ratios (wt:wt) upon SVA treatment with different Tol volumes.

D:A	SVA (65 s)	V_{OC} (V)	J_{SC} (mA·cm^{-2})	FF (%)	PCE[a] (%)
1:1	300μl	0.99	17.27	57.0	9.52 (9.31)
	500μl	1.00	16.07	57.6	9.08 (8.79)
	700μl	0.99	15.63	58.6	8.92 (8.73)
1:0.75	300μl	0.99	15.72	61.2	9.57 (9.39)
	500μl	0.99	16.84	60.2	10.08 (9.87)
	700μl	1.00	16.72	56.6	9.44 (9.22)
1:0.5	300μl	1.01	16.32	61.1	9.86 (9.65)
	500μl	1.02	14.28	63.1	8.97 (8.75)
	700μl	1.02	14.78	63.0	9.29 (9.04)

[a] Optimal and statistical results are listed outside of parentheses and in parentheses, respectively. The average values are obtained from over 20 devices.

Table S4 The detailed photovoltaic performance of OSCs based on DRTT-R:F-2Cl (1:0.75) with 150μl CF annealing for different time.

treatment time (s)	V_{OC} (V)	J_{SC} (mA·cm^{-2})	FF (%)	PCE[a] (%)
70	1.00	14.95	51.6	7.74 (7.55)
80	0.98	14.82	60.2	8.72 (8.49)
90	0.97	15.11	59.5	8.70 (8.46)

[a] Optimal and statistical results are listed outside of parentheses and in parentheses, respectively. The average values are obtained from over 20 devices.

Table S5 The detailed photovoltaic performance of OSCs based on DRTT-T:F-2Cl (1:0.75) upon SVA treatment with different Tol volumes.

SVA (65 s)	V_{OC} (V)	J_{SC} (mA·cm^{-2})	FF (%)	PCE[a] (%)
300μl	1.04	14.38	47.4	7.09 (6.82)
500μl	1.04	15.10	51.3	8.06 (7.79)
700μl	1.01	14.36	39.8	5.78 (5.56)

[a] Optimal and statistical results are listed outside of parentheses and in parentheses, respectively. The average values are obtained from over 20 devices.

Table S6 The detailed photovoltaic performance of OSCs based on DRTT-T:F-2Cl (1:0.75) with 150μl CF annealing for different time.

treatment time (s)	V_{OC} (V)	J_{SC} (mA·cm^{-2})	FF (%)	PCE[a] (%)
70	0.96	15.75	61.8	9.37 (9.15)
80	0.95	15.72	62.8	9.37 (9.18)
90	0.95	14.63	59.6	8.31 (8.12)

[a] Optimal and statistical results are listed outside of parentheses and in parentheses, respectively. The average values are obtained from over 20 devices.

Table S7 The detailed photovoltaic performance of OSCs based on DRTT-T:F-2Cl and DRTT-R:F-2Cl with different active layer thicknesses. DRTT-T:F-2Cl and DRTT-R:F-2Cl films were treated with CF and Tol SVA, respectively.

Donor	Thickness (nm)	V_{OC} (V)	J_{SC} (mA·cm^{-2})	FF (%)	PCE[a] (%)
DRTT-T	100	0.96	15.33	63.1	9.26 (9.05)
	120	0.95	15.72	62.8	9.37 (9.18)
	150	0.94	15.65	56.2	8.23 (8.06)
DRTT-R	100	1.01	15.80	61.1	9.74 (9.51)
	120	1.00	16.82	62.6	10.45 (10.23)
	150	1.01	15.52	59.6	9.30 (9.11)

[a] Optimal and statistical results are listed outside of parentheses and in parentheses, respectively. The average values are obtained from over 20 devices.

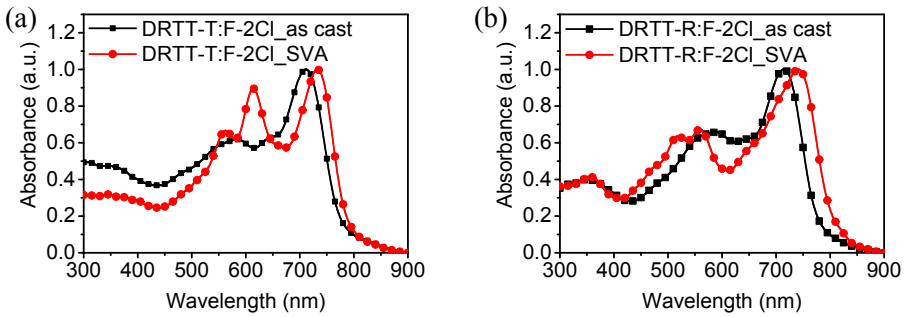

Fig. S28 Absorption spectra of THF-processed DRTT-T:F-2Cl (a) and DRTT-R:F-2Cl (b) blend films without and with SVA treatment. Donor:acceptor weight ratio: 1:0.75.

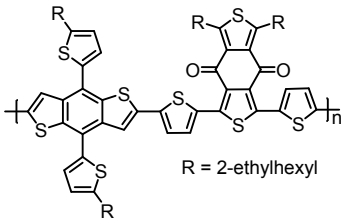

Fig. S29 Chemical structure of PBDB-T.

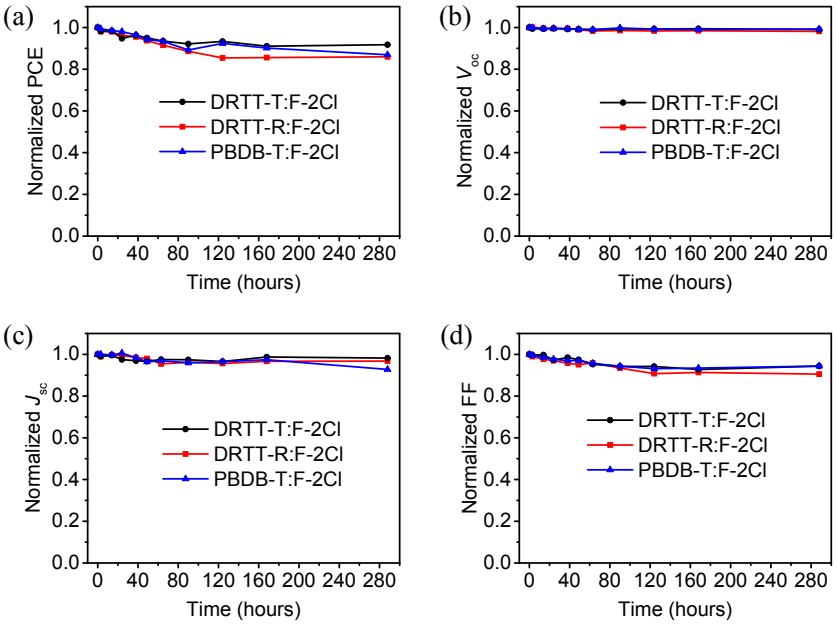

Fig S30 Normalized photovoltaic parameters for DRTT-T:F-2Cl, DRTT-R:F-2Cl and PBDB-T:F-2Cl based OSCs in an argon-filled glove box. The temperature of the devices is around 30 °C.

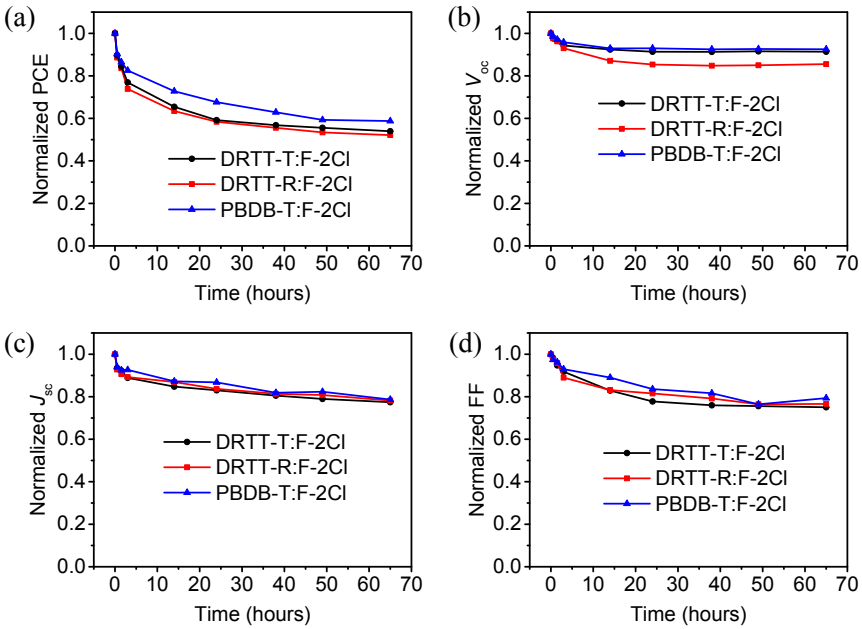

Fig S31 Normalized photovoltaic parameters versus continuous illumination (AM 1.5G, 100 mW/cm^2) time for DRTT-T:F-2Cl, DRTT-R:F-2Cl and PBDB-T:F-2Cl based OSCs in an argon-filled glove box. The temperature of the devices under the lamp is around 50 °C.

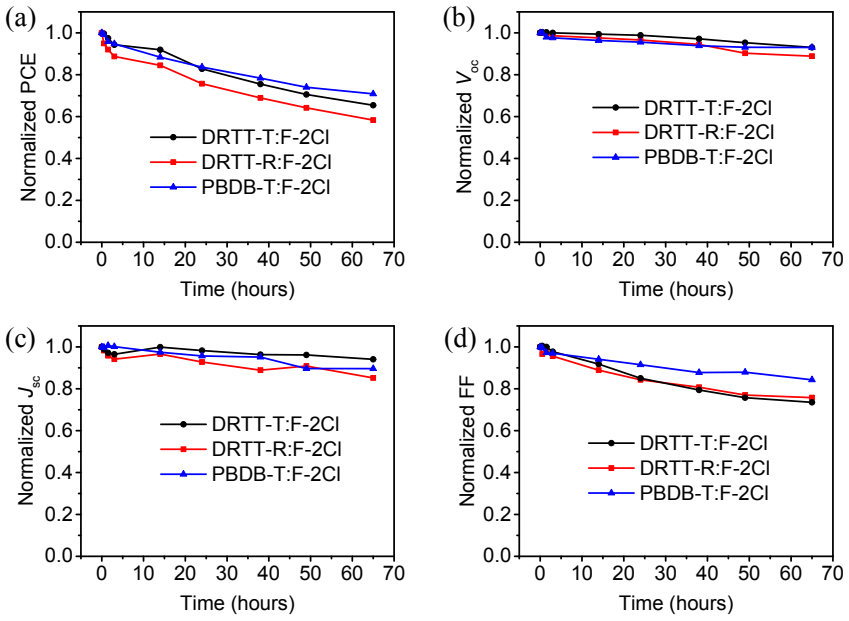

Fig S32 Normalized photovoltaic parameters versus continuous heating time for DRTT-T:F-2Cl, DRTT-R:F-2Cl and PBDB-T:F-2Cl based OSCs at 60 °C in an argon-filled glove box.

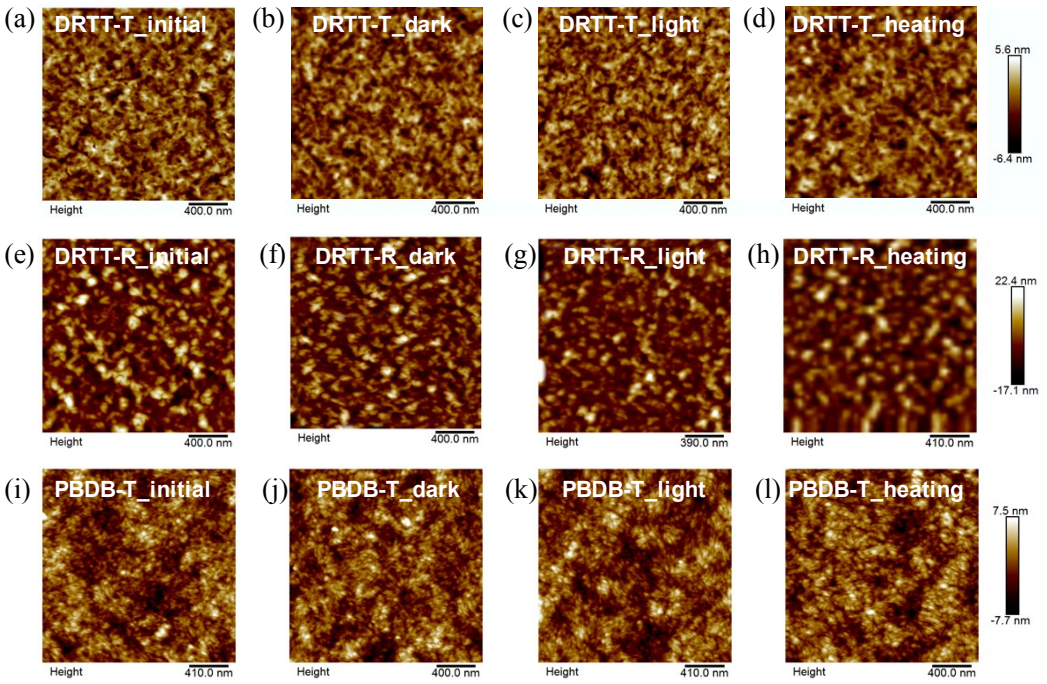

Fig S33 AFM images of DRTT-T:F-2Cl (a-d), DRTT-R:F-2Cl (e-h) and PBDB-T:F-2Cl (i-l) blend films after keeping in an argon-filled glove box for 168 h (b, f, j), and continuous illumination (c, g, k) and heating for 65 h (d, h, l).

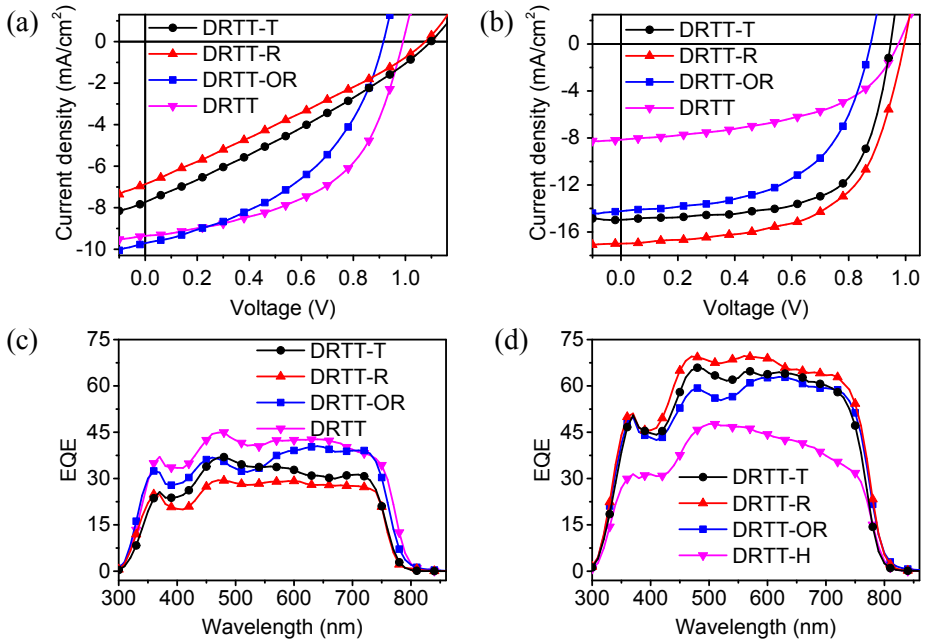

Fig. S34 Current density-voltage (*J-V*) characteristics (a, b) and the external quantum efficiency (EQE) curves (c, d) of the OSCs based donor:F-2Cl with CF as processing solvent without (a, c) and with (b, d) SVA treatment.

Table S8 The detailed photovoltaic performance of OSCs based on DRTT-OR:F-2Cl (1:0.75) and DRTT:F-2Cl (1:0.75) with different treatments.

donor	treatment	V_{OC} (V)	J_{SC} (mA·cm^{-2})	FF (%)	PCE[a] (%)
DRTT-OR	500μl Tol 65s	0.88	14.23	55.6	6.95 (6.71)
	150μl CF 80s	0.87	13.98	57.1	6.95 (6.74)
DRTT	500μl Tol 65s	0.97	8.15	50.4	4.00 (3.71)
	150μl CF 80s	0.97	7.51	51.5	3.77 (3.52)

[a] Optimal and statistical results are listed outside of parentheses and in parentheses, respectively. The average values are obtained from over 20 devices.

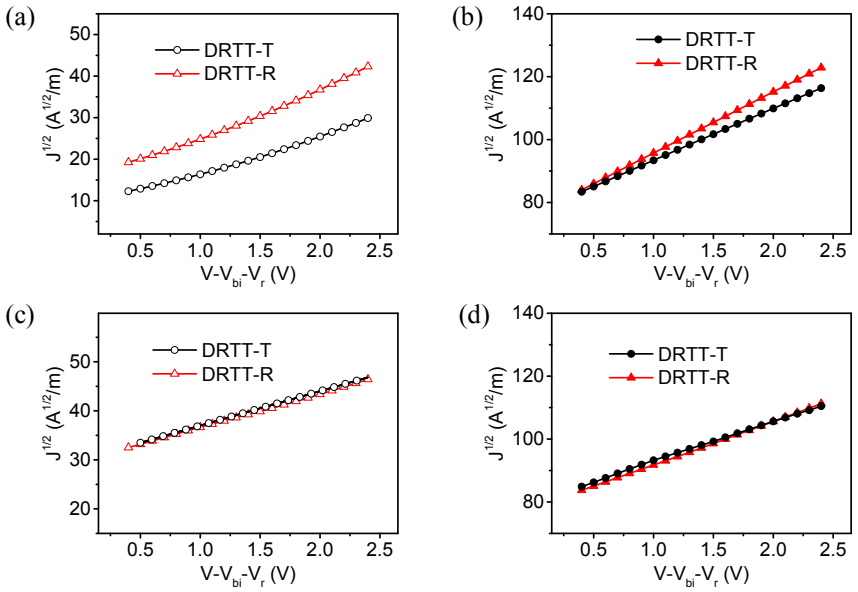

Fig. S35 *J-V* characteristics for the hole-only (a, b) and electron-only (c, d) devices based on the THF-processed blend films. The solid lines represent the fit using a model of single carrier SCLC with field-independent mobility.

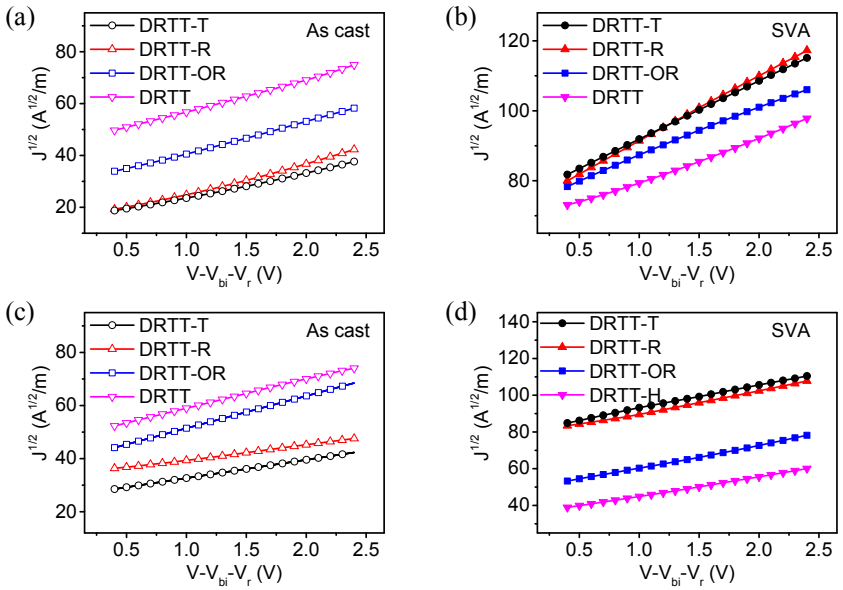

Fig. S36 *J-V* characteristics for the hole-only (a, b) and electron-only (c, d) devices based on the CF-processed blend films. The solid lines represent the fit using a model of single carrier SCLC with field-independent mobility.

Table S9 Mobility results of SCLC devices based on donor:F-2Cl blend films.

Donor	Solvents	Treatment	μ_h[a] (10^{-4} cm^2 V^{-1} s^{-1})	μ_e[a] (10^{-4} cm^2 V^{-1} s^{-1})	μ_h/μ_e[b]
DRTT-T	THF	As cast	0.65 (0.55±0.08)	0.37 (0.26±0.10)	1.76
		SVA[d]	2.12 (2.01±0.09)	1.40 (1.29±0.09)	1.51
DRTT-R	THF	As cast	0.99 (0.85±0.11)	0.34 (0.25±0.06)	2.91
		SVA[c]	2.80 (2.71±0.07)	1.44 (1.32±0.09)	1.94
DRTT-T	CF	As cast	0.68 (0.60±0.06)	0.38 (0.26±0.10)	1.79
		SVA[d]	2.10 (2.01±0.08)	1.44 (1.35±0.06)	1.46
DRTT-R	CF	As cast	0.98 (0.88±0.08)	0.25 (0.15±0.07)	3.92
		SVA[c]	2.54 (2.44±0.07)	1.42 (1.32±0.08)	1.79
DRTT-OR	CF	As cast	1.06 (0.92±0.11)	1.06 (0.95±0.09)	0.98
		SVA[c]	1.37 (1.25±0.09)	1.15 (1.02±0.10)	1.19
DRTT	CF	As cast	1.13 (1.04±0.07)	1.06 (0.92±0.11)	1.07
		SVA[c]	1.13 (1.06±0.05)	0.89 (0.78±0.08)	1.27

[a] Optimal and statistical results are listed outside of parentheses and in parentheses, respectively. The average values are obtained from over 15 devices. [b] μ_h/μ_e calculated from the optimal μ_h and μ_e. [c] The SVA treatment was conducted with Tol for 65 s. [d] The SVA treatment was conducted with CF for 80s.

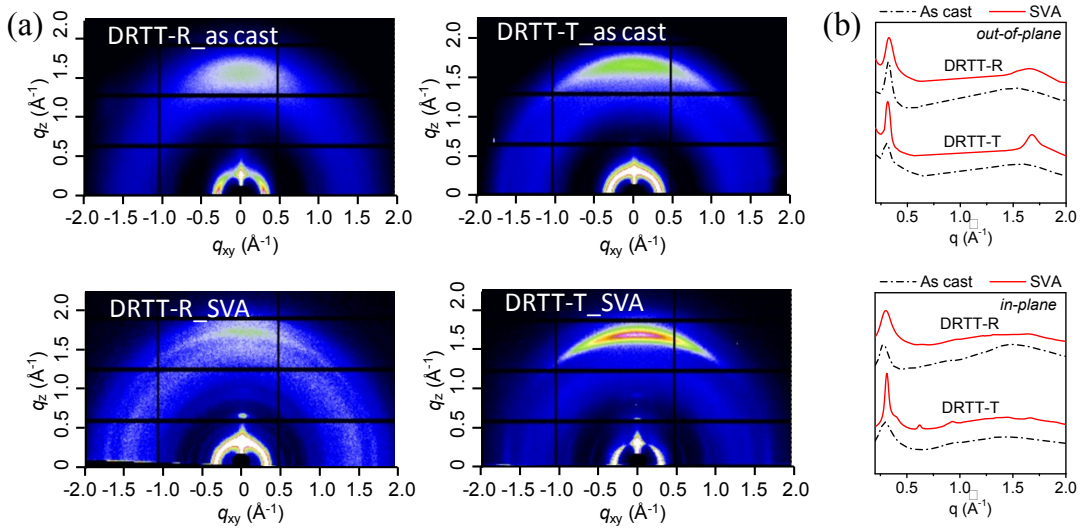

Fig S37 2D-GIWAXS patterns (a) of DRTT-T and DRTT-R neat films processed with THF under different conditions, and the out-of-plane and the in-plane GIWAXS profiles (b) derived from (a).

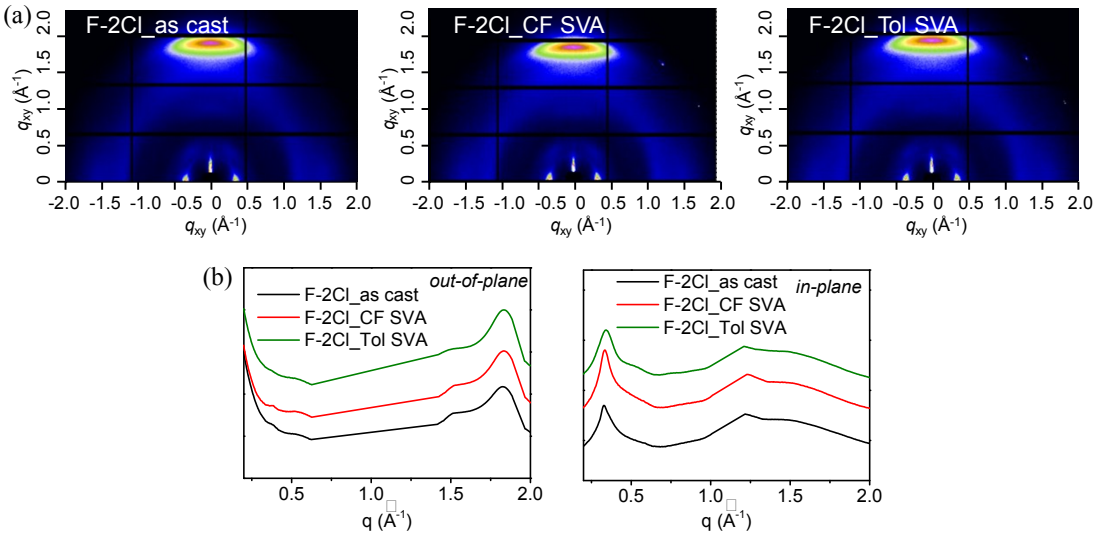

Fig S38 2D-GIWAXS patterns (a) of F-2Cl neat films processed with THF under different conditions, and the out-of-plane and the in-plane GIWAXS profiles (b) derived from (a).

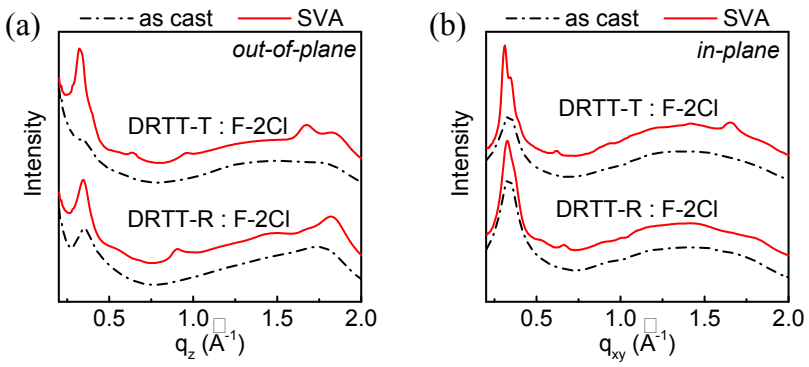

Fig. S39 The out-of-plane (a) and the in-plane (b) GIWAXS profiles derived from 2D-GIWAXS patterns of DRTT-T:F-2Cl and DRTT-R:F-2Cl blend films processed with THF.

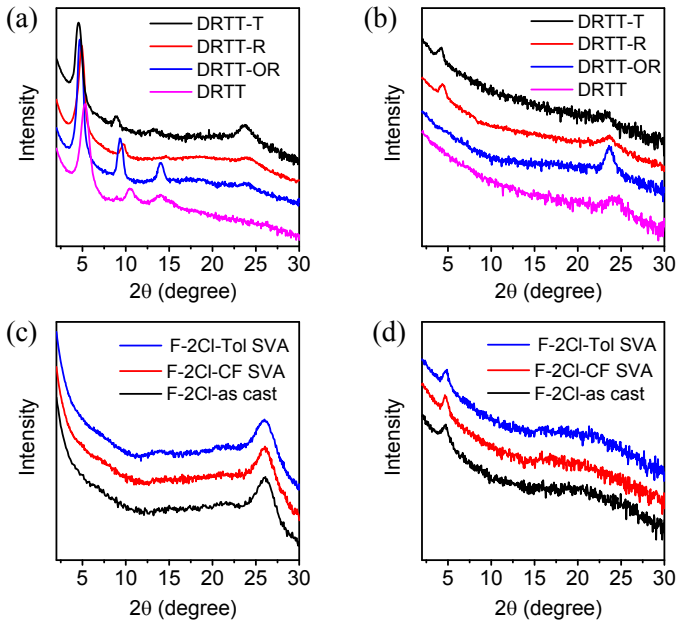

Fig. S40 Out-of-plane (a, c) and in-plane (b, d) XRD patterns of DRTT-T, DRTT-R, DRTT-OR, DRTT and F-2Cl neat films with the same SVA treatment as device optimization.

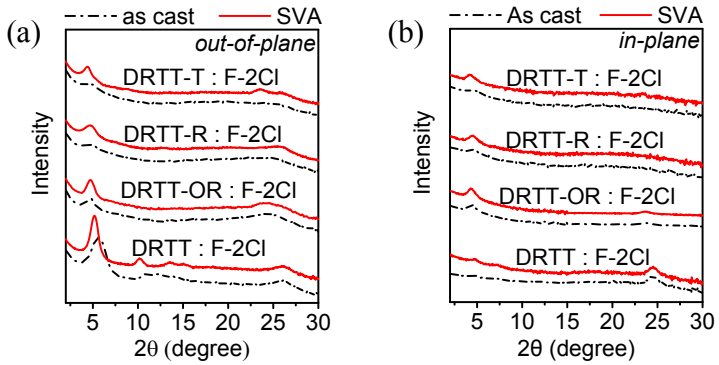

Fig. S41 Out-of-plane (a) and in-plane (b) XRD patterns of DRTT-T:F-2Cl, DRTT-R:F-2Cl, DRTT-OR:F-2Cl and DRTT:F-2Cl blend films processed with CF.

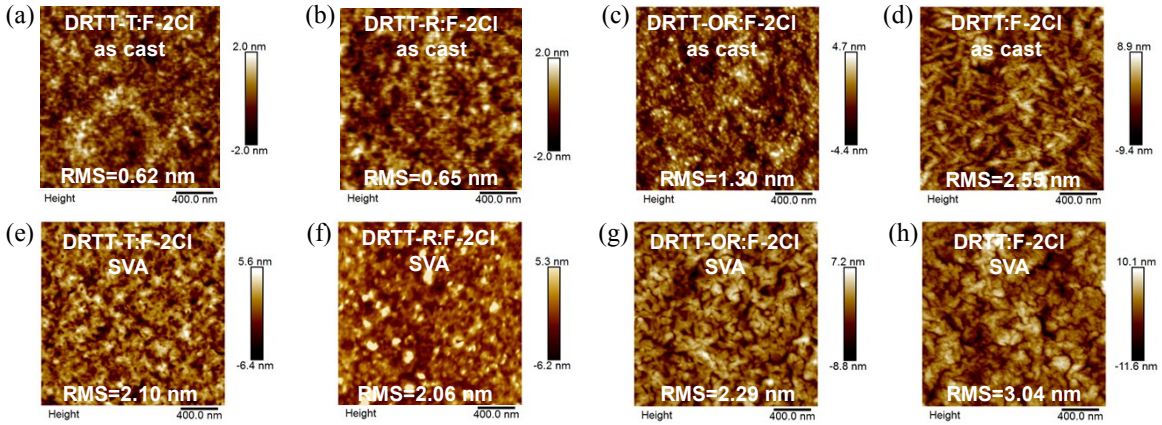

Fig S42 AFM images of DRTT-T:F-2Cl, DRTT-R:F-2Cl, DRTT-OR:F-2Cl and DRTT:F-2Cl blend films processed with CF.

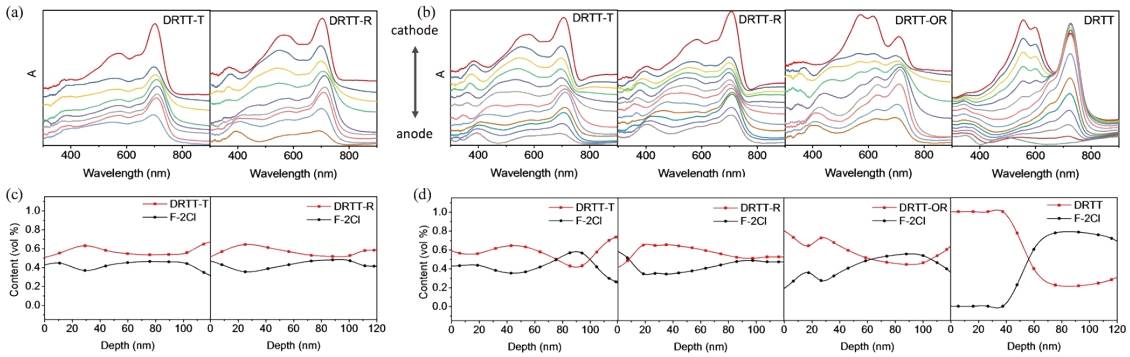

Fig S43 Film-depth-dependent light absorption spectra of the pristine blend films processed with THF (a) and CF (b), and distribution of donor and acceptor in the pristine blend films processed with THF (c) and CF (d) along the vertical direction. For clarity, the spectra in (a) and (b) have been vertically relocated, and each spectrum corresponds to a sublayer with thickness ca. 10 nm. (c) and (d) were obtained from (a) and (b), respectively.

References

1 Y. Wang, Y. Wang, B. Kan, X. Ke, X. Wan, C. Li, Y. Chen, *Adv. Energy Mater*., 2018, **8**, 1802021.

2 N. Hergue, P. Frere, J. Roncali, *Org. Biomol. Chem.,* 2011, **9**, 588.

3 M. Landman, M. van Staden, H. Görls, S. Lotz, *Inorg. Chim. Acta.,* 2005, **358**, 2602.

4 M. Sato, A. Asami, G. Maruyama, M. Kosuge, J. Nakayama, S. Kumakura, T. Fujihara, K. Unoura, *J. Organomet. Chem.,* 2002, **654**, 56.